Journal of Iberian Geology
https://doi.org/10.1007/s41513-025-00288-8

RESEARCH PAPER

Magnetic fabrics of weakly-deformed mudrocks from the Jaca-Pamplona basin (Pyrenees); new constrains on the sensitivity of magnetic fabrics and the tectonic evolution of the Southern Pyrenees

P. Sierra-Campos[1,2] · P. Calvín[1,2] · E. Izquierdo-Llavall[1,2] · J. I. Pérez-Landazabal[3] · M. Montes[4] · A. Luzón[2,5] · E. Bellido[4] · E. L. Pueyo[1,2] · J. C. Larrasoaña[1,2,3]

Received: 21 May 2024 / Accepted: 11 February 2025

Abstract

The anisotropy of magnetic susceptibility (AMS) is a sensitive marker for studying the spatial and temporal evolution of orogens. In weakly deformed rocks deposited in compressive contexts the AMS signal mostly reflects the preferential alignment and deformation of paramagnetic phyllosilicates during early layer parallel shortening (LPS) related to both near and/or far-field structures. Moreover, localized deformation and post-depositional shearing in the vicinity of thrusts can alter early LPS fabrics. An AMS analysis of 651 samples was conducted along two stratigraphic sections, Izaga and Berdún (2800 m-thick), in the Jaca-Pamplona basin (Southern Pyrenees). The sampled sections record the tectonosedimentary evolution of the basin from the Late Lutetian to the Middle Priabonian. In both sections, the magnetic fabric is controlled by LPS. The lower and upper part of the Izaga section shows triaxial to oblate and oblate ellipsoids, respectively, which are interpreted to indicate a decrease of tectonic activity associated to the Larra thrust system. The Berdún section begins with oblate ellipsoids, which subsequently become triaxial and prolate before returning oblate towards the top of the succession. Ellipsoids in the lower part of the section exhibit an incipient girdle between the minimum and intermediate axes, which signal an undetected thrust, further corroborated, by structural analysis. The remainder of the Berdún section shows a magnetic fabric derived from LPS but it is not possible to associate it to any structure. The uppermost part of the section displays prolate ellipsoids, which we link to enhanced tectonic activity leading to continentalization of the basin.

Keywords Magnetic fabrics · Layer parallel shortening · Weakly-deformed mudrocks · Thrusting · Jaca-Pamplona basin · Pyrenees

✉ P. Sierra-Campos
p.sierra@igme.es

P. Calvín
p.calvin@igme.es

E. Izquierdo-Llavall
e.izquierdo@igme.es

J. I. Pérez-Landazabal
ipzlanda@unavarra.es

M. Montes
m.montes@igme.es

A. Luzón
aluzon@unizar.es

E. Bellido
e.bellido@igme.es

E. L. Pueyo
unaim@igme.es

J. C. Larrasoaña
jc.larra@igme.es

1 CN IGME, CSIC, Unidad de Zaragoza, 50059 Zaragoza, Spain

2 Unidad Asociada en Ciencias de la Tierra IGME-Universidad de Zaragoza, Zaragoza, Spain

3 Dpto. Ciencias, Universidad Pública de Navarra, 31006 Pamplona, Navarra, Spain

4 CN IGME, CSIC, 28760 Tres Cantos, Madrid, Spain

5 Dpto. Ciencias de la Tierra, Facultad de Ciencias, Universidad de Zaragoza, 50009 Zaragoza, Spain

Published online: 03 March 2025

Resumen

La anisotropía de la susceptibilidad magnética (ASM) es una técnica que se ha mostrado muy eficiente en el estudio de la evolución tectónica de cinturones orogénicos. En rocas débilmente deformadas depositadas en contextos compresivos, la ASM viene marcada por la orientación preferente de filosilicatos paramagnéticos ocurrida durante la diagénesis inicial como respuesta al acortamiento paralelo a las capas (LPS). Estas fábricas asociadas al LPS pueden verse modificadas con posterioridad como respuesta al cizallamiento en la cercanía de planos de cabalgamiento. En este trabajo se presenta el análisis de la ASM en dos secciones, Izaga y Berdún, que se sitúan en la cuenca de Jaca-Pamplona (Zona Surpirenaica) y registran la evolución tectonosedimentaria de la cuenca desde el Luteciense Superior al Priaboniense Medio. Las partes inferior y superior de la serie de Izaga muestran elipsoides triaxiales/oblatos y oblatos, respectivamente, que indican un decaimiento en la intensidad del LPS asociado a la actividad decreciente del lejano sistema de cabalgamientos de Larra. La sección de Berdún comienza con elipsoides oblatos, que cambian rápidamente a triaxiales y prolatos antes de volver a oblatos hacia la parte media y superior de la serie. Los elipsoides triaxiales y prolatos en la parte baja de la serie marcan, junto con el desarrollo de una guirnalda incipiente entre los ejes mínimos e intermedios de la ASM, el efecto adicional de un cizallamiento que relacionamos con un cabalgamiento no detectado anteriormente y cuya presencia ha sido corroborada por análisis estructural. Aunque el resto de la serie de Berdún refleja el efecto del LPS, no ha sido posible determinar si éste viene condicionado por una estructura cercana o lejana. Los elipsoides prolatos reaparecen en el techo de la serie, circunstancia que relacionamos con un LPS más intenso asociado a la actividad tectónica que condicionó continentalización de la cuenca.

.

Palabras clave Fábricas magnéticas · Acortamiento paralelo a las capas · Rocas débilmente deformadas · Cabalgamientos · Cuenca de Jaca-Pamplona · Pirineos

1 Introduction

The anisotropy of magnetic susceptibility (AMS) has become a standard tool in tectonic studies given its ability to delineate the strain-related preferred orientation of phyllosilicates within mudrocks that show no macroscopic evidence for deformation (Graham, 1954; Nye, 1957; Tarling & Hrouda, 1993; Borradaile & Henry, 1997; Borradaile, 2001; Borradaile & Jackson, 2004, 2010). This ability emerges from the spatial correlation reported between the magnetic and the crystallographic anisotropy of these minerals (e.g., Martín-Hernández & Hirt, 2003). Mudstones that have been affected by compaction and are tectonically undeformed are characterised by a sedimentary fabric in which the maximum (k_{max}) and intermediate (k_{int}) axes of an oblate magnetic ellipsoid are scattered within the bedding plane, being the minimum axis (k_{min}) perpendicular to the bedding. This type of fabric is commonly referred in the literature as Type I (Larrasoaña et al., 2004; Soto et al., 2009; Parés, 2015). Magnetic fabrics in seemingly undeformed mudstones are sensitive enough to record the syn-sedimentary strain, whether in extensional (e.g. Cifelli et al., 2004; García-Lasanta et al., 2013) or compressional contexts (Parés et al., 1999; Caricchi et al., 2016). In compressional settings, such as fold-and-thrust belts and their related foreland basins, phyllosilicates are first aligned perpendicular to syn-sedimentary layer-parallel shortening (LPS), leading to the development of a so-called Type IIa fabric (Parés, 2015). This magnetic fabric is characterized by a magnetic lineation (defined by k_{max} axes) perpendicular to the shortening direction, while the magnetic foliation remains parallel to bedding. An increase in deformation results in the formation of pencil structures and, subsequently, of a weak cleavage. This is evidenced by triaxial to prolate magnetic fabrics with enhanced clustering of magnetic lineation and the development of a girdle between the intermediate and minimum magnetic axes (Type IIb of Parés, 2015), showing the competition between bedding and cleavage in the control of magnetic foliation (Pueyo-Anchuela et al., 2012a). If deformation progresses to the point of reaching strong cleavage development, the degree of anisotropy increases with the development of a magnetic foliation that is parallel to the cleavage plane, at the same time that k_{max} either remains parallel to the intersection lineation between cleavage and bedding or distributes within the cleavage plane (Type III of Parés, 2015). Due to these deformation-related changes, the AMS has been proven as a very sensitive marker for studying both the spatial and the temporal evolution of strain in orogens and foreland basins (Borradaile & Henry, 1997; Parés, 2004, 2015; Pueyo-Anchuela et al., 2011). The sensitivity is such that AMS results from mudrocks have been used even to detect blind or cryptic faults that, given the homogeneous nature of most marly sequences, can escape from visual inspection during field work. In these cases, magnetic fabrics record strong deformation gradients ranging from bedding- to cleavage-parallel foliations in short distances from the thrust surface (typically < 1 km), where regional AMS patterns are obliterated by the local effect of thrusting (Hirt et al., 2004; Boiron et al., 2020; Gracia-Puzo et al., 2021; Menzer et al., 2024).

The Jaca-Pamplona basin is an E-W-trending basin filled by Eocene–Oligocene syn-tectonic marine and continental sediments that record the early stages in the evolution of the south-Pyrenean foreland (Garcés et al., 2020; Fig. 1a, b). In early shortening stages, the Jaca-Pamplona basin developed at the footwall of basement thrusts located to the north, in the internal part of the mountain belt (e.g., the Lakora-Eaux-Chaudes thrust; Labaume et al., 2016b and references therein). These early basement thrusts transferred shortening into the overlying sedimentary cover (e.g., the Larra thrust system; Labaume et al., 1985, 2016b; Teixell, 1992, 1996). As basement deformation migrated southwards, either from Bartonian-Priabonian (Labaume et al., 2016a, 2016b) or Lutetian times (Séguret, 1972; Fernández et al., 2012; Muñoz et al., 2013), the Gavarnie basement thrust led to the folding of the overlying Larra thrust system and a regional-scale cleavage domain developed in the northernmost fringe of the Jaca-Pamplona basin (Labaume et al., 1985; Tavani et al., 2006; Izquierdo-Llavall et al., 2013). The basin was eventually transported southwards, and exhumed, as a piggy-back basin above of the Guarga basement thrust. Again, uncertainty exists on the chronology of this thrusting, with some authors indicating a Late Rupelian to Aquitanian age (Millán et al., 2000; Labaume & Teixell, 2018) while others advocate for an earlier (Late Eocene-Early Rupelian) timing (Fernández et al., 2012; Muñoz et al., 2013, 2018).

Magnetic fabrics of Ypresian to Priabonian marine mudrocks have been systematically studied across the Jaca-Pamplona basin over the last two decades (Pueyo-Morer et al., 1997; Larrasoaña et al., 2004; Oliva-Urcia et al., 2009; Pueyo-Anchuela et al., 2010, 2011, 2012a, 2012b). These studies point, as has been summarized by Pocoví et al. (2014), to a model in which incipient tectonic fabrics in the northern part of the basin developed in response to shortening along the Lákora-Eaux-Chaudes, Larra and Gavarnie thrust systems, which manifested in the area as a far-field LPS. As deformation progressed in a piggy-back sequence, the imprint of this LPS migrated southwards accordingly (affecting the southern part of the Jaca-Pamplona basin), whereas it was overprinted in the northernmost part of the basin by the formation of the cleavage domain. In the latest years, new thrust units involving the basement are being identified from *vintage* exploration seismic sections at an intermediate position between the Gavarnie and Guarga thrust units (Labaume et al., 2016b; Labaume & Teixell, 2018; Izquierdo-Llavall et al., 2023). These units are buried below the thick sedimentary succession of the Jaca-Pamplona basin but in some exceptional locations, such as the Leire and Illón ranges, that provoke a significant uplift of cover sequences at their hanging-walls (Izquierdo-Llavall et al., 2023). The location of these basement thrust units at an intermediate position of the basin demands a reassessment of the significance of the magnetic fabrics studied in the area so far. In this tectonic scenario, what has been classically considered as a far-field effect of the internal thrust units of the belt (e.g., the Lákora-Eaux-Chaudes, Larra and Gavarnie systems), might have been caused by more proximal/local structures, thereby claiming for a change in our perception of the sensitivity of magnetic fabrics to Pyrenean deformation and its evolution.

This paper introduces the AMS results from two Eocene stratigraphic sections, named Izaga and Berdún, which have been sampled in the central sector of the Jaca-Pamplona basin at the footwall of the Illón and Leire thrust systems, respectively, and away from the regional cleavage domain located to the North. As opposed to previous studies, which have been based on the collection of standard magnetic fabric sites distributed across the basin according to outcrop availability, this work presents the study of magnetic fabrics along two stratigraphic successions located at a specific position with respect to tectonic structures of special interest. These sections provide a singular opportunity to constrain the sensitivity of magnetic fabrics to compression over time, and to shed light on the evolution of the Jaca-Pamplona basin in the context of the Pyrenean range. To achieve this, it is essential to tie these magnetic fabrics to their putative causing structures.

2 Geological setting

The Pyrenees constitute a doubly-verging orogen formed by the collision between the Iberian and Eurasian plates between the Late Cretaceous and the Early Miocene (Choukroune, 1992; Muñoz, 1992, 2002; Teixell, 1996). From north to south, the Pyrenees are divided into three along-strike domains, namely the North Pyrenean, the Axial and the South Pyrenean zones (Fig. 1a). The study area is located in the central sector of the South Pyrenean Zone (SPZ), which is bounded to the North by the Palaeozoic units of the Axial Zone and thrusts to the south onto the Cenozoic units of the Ebro foreland basin. Both the Axial and the South Pyrenean zones are characterized by a dominant southwards vergence. N–S geological cross-sections over the study area (Fig. 1c) illustrate the tectonic architecture of the Axial and SPZ zones, which are interpreted to be formed by three main basement-involved structures that, from north to south, correspond to the Lakora-Eaux-Chaudes, Gavarnie, and Guarga thrusts (Teixell, 1998; Millán et al., 2000). In addition to these three main basement thrusts, the Roncal well (Lanaja, 1987; see location in Fig. 1c) drilled a basement anticline in the footwall of the Gavarnie thrust, which has been interpreted as the hangingwall anticline of an additional, south-directed basement thrust that was depicted in the geological cross-sections by Labaume et al. (1985), Teixell (1996) and Teixell et al. (2016), and is named as Gavarnie-2 in

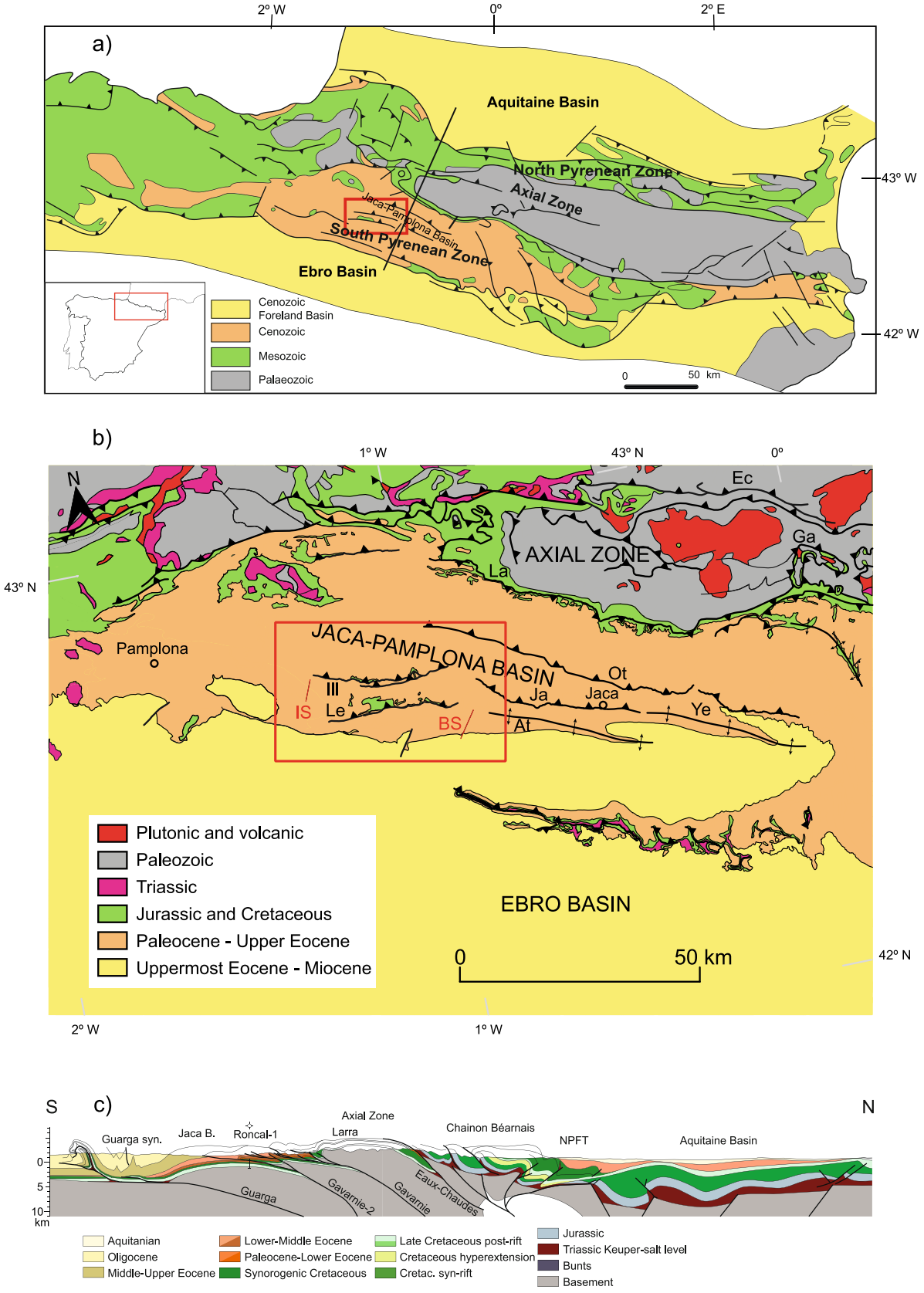
a)
2° W
0°
2° E
43° W
42° W
Aquitaine Basin
North Pyrenean Zone
Axial Zone
Jaca-Pamplona Basin
South Pyrenean Zone
Ebro Basin
Cenozoic Foreland Basin
Cenozoic
Mesozoic
Palaeozoic
0
50 km
b)
1° W
43° N
0°
N
Ec
Ga
AXIAL ZONE
La
43° N
Pamplona
JACA-PAMPLONA BASIN
Ot
Ja
Jaca
Ye
III
IS
Le
BS
At
Plutonic and volcanic
Paleozoic
Triassic
Jurassic and Cretaceous
Paleocene - Upper Eocene
Uppermost Eocene - Miocene
EBRO BASIN
0
50 km
42° N
2° W
1° W
c)
S
N
Axial Zone
Guarga syn.
Jaca B.
Roncal-1
Larra
Chainon Béarnais
NPFT
Aquitaine Basin
0
5
10
km
Guarga
Gavarnie-2
Gavarnie
Eaux-Chaudes
Aquitanian
Oligocene
Middle-Upper Eocene
Lower-Middle Eocene
Paleocene-Lower Eocene
Synorogenic Cretaceous
Late Cretaceous post-rift
Cretaceous hyperextension
Cretac. syn-rift
Jurassic
Triassic Keuper-salt level
Bunts
Basement

◂**Fig. 1** **a** Geological map of the Pyrenees (modified from Teixell, 1996) with location of the study area location (red box). **b** Geological map of the southern Pyrenees with the main structures with the study area (red box); Ec: Eaux-Chaudes thrust; Ga: Gavarnie thrust; La: Larra thrust; Ot: Oturia thrust; Ja: Jaca thrust; Ill: Illón thrust; Le: Leire thrust; Ye: Yebra de Basa anticline; At: Atarés anticline. **c** Geological cross-section along the study area (NE–SW black line in **a**) (modified from Pedrera et al., 2023)

Saspiturry et al. (2019). These basement structure transfer shortening to cover units (Fig. 1a–c) where folding and thrusting are controlled by the existence of two main décollements (e.g., Labaume et al., 1985; Teixell, 1996; Izquierdo-Llavall et al., 2013), the Late Cretaceous marls of the Zuriza Formation, along which the Larra system is detached, and the Late and the Middle Triassic evaporites of the Keuper and Muschelkalk units, along which the Guarga unit shows a main thrust flat that separates the Jaca-Pamplona basin from the Ebro foreland basin to the South.

Knowledge on the timing of thrusting comes from a combination of tectono-sedimentary relations recorded by growth strata and angular unconformities and from thermochronological data (e.g., Labaume et al., 1985, 2016a, 2016b; Teixell, 1996; Jolivet et al., 2007; Rahl et al., 2011; Muñoz et al., 2013; Abd Elmola et al., 2018; Labaume & Teixell, 2018). These observations have been done in different areas along the strike of the Jaca-Pamplona basin and have led to a range of potential thrusting ages, with basement deformation timing ranging from Ypresian to Bartonian, Lutetian to Rupelian, and Early Rupelian to Aquitanian times for the Lákora-Eaux-Chaudes, Gavarnie and Guarga thrust sheets, respectively (Fig. 2) (see age discussion in Labaume et al., 2016a, 2016b). Even though the absolute age of basement deformation is a matter of debate, general agreement exists on the relative timing of basement thrusting following a piggy-back sequence.

Since sedimentation occurred simultaneously to the southward migration of tectonic activity, these thrust systems affected younger sedimentary sequences moving progressively towards the south. Thus, activity of the Larra system was broadly coeval with deposition of most of the Hecho Group in a submarine fan along an E-W oriented foredeep that was fed axially from the already uplifting areas of the Central Pyrenees. This turbiditic sequence interbeds up to nine levels of carbonate megabreccia and grade upwards to prodeltaic units (Larrés and Sabiñanigo-Urroz formations) related to the progressively southwards migration of deformation (Labaume et al., 1983, 2016a, 2016b; Mutti, 1991; Payros et al., 1999). Later displacement of the Gavarnie thrust witnessed the continued westward progradation of a sedimentary sequence composed by prodeltaic marls (Pamplona Formation) and transitional sediments (Belsué-Atarés and Guendulain formations). Later sedimentation is related to continental environments leading to deposition of the Campodarbe and Uncastillo formations, which record the southward transport of the basin atop the Guarga thrust from Priabonian to Aquitanian times, giving form to the final architecture of the South Pyrenean sole thrust in the External Sierras front (Millán et al., 1995, 2000).

The studied area, in the central sector of the Jaca-Pamplona basin, is characterized by the occurrence of two south-directed cover thrust units (the Illón and Leire thrust) located to the South of the Gavarnie-2 basement thrust (Fig. 1b, c). The Illón and Leire thrusts display an E–W orientation, extend ~ 20 km along-strike, and bring Late Cretaceous to Eocene carbonate rocks onto the Lutetian turbidites of the Hecho Group and the Bartonian-Priabonian marls of the Larrés, Urroz and Pamplona formations (Figs. 3, 4). Different depth geometries have been proposed for these thrust units, which have been interpreted either as fault-bend folds detached over a thin layer of Keuper evaporites (Labaume et al., 1985; Teixell, 1996; Teixell et al., 2016) or as detachment folds cored by a thick Keuper sequence and affected by south-directed thrusts (Oliva-Urcia et al., 2012; Saspiturry et al., 2019). These two interpretations consider the Illón and Leire thrusts as cover structures fully decoupled from the underlying basement, although recent seismic interpretations suggest that the basement underneath the system is also affected by thick-skinned thrusting (Toro et al., 2021). Geological maps in the area evidence key onlaps and thickness variations in syn-tectonic units that provide significant constraints on the Illón and Leire thrust emplacement ages (see Sect. 4.1).

3 Materials and methods

3.1 Studied magnetostratigraphic profiles and geological cross-sections

The Izaga section (base: 42° 42′ 37.95″ N, 1° 15′ 43.12″’ W; top: 42° 41′ 49.57″ N, 1° 17′ 12.42″ W) was sampled in the badlands near the village of Nardués-Andurra, in the northern limb of the eastern termination of the Izaga syncline, ~ 3 to 8 km south of the Illón thrust (Fig. 3). A total of 173 evenly distributed sites were sampled along a 1116 m-thick section that encompass the uppermost 450 m of the Hecho Group (including the uppermost megabreccia identified in the area), the Larrés (500 m-thick) and Urroz (110 m-thick) formations, and the lowermost 50 m of the Pamplona Formation (Fig. 3). These rocks display a constant SSW dip of about 30° throughout the section. Their age (ca. 42–40 Ma) is constrained by biostratigraphic data based on planktonic foraminifera (Payros et al., 1999), which indicate a Late Lutetian age for the uppermost Hecho Group and the lower part of the Larrés Formation, and an Early Bartonian age for the upper half of the Larrés Formation, the Urroz Formation

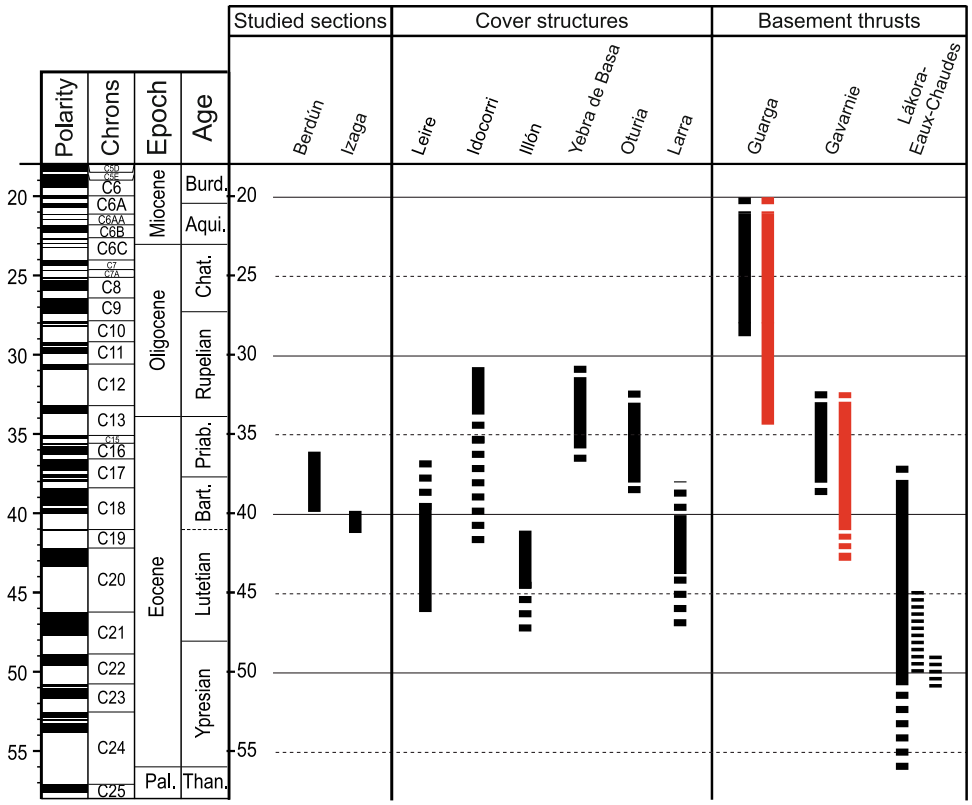

Fig. 2 Thrusts activity (in black ages in Labaume et al., 2016b; in red ages in Fernández et al., 2012 and in Muñoz et al., 2013, 2018) (modified from Labaume et al., 2016b). The ages of the studied sections according to available chronostratigraphic data (Gonzalvo, 1992, 1997; Payros et al., 1999; Oms et al., 2003; Vinyoles et al., 2021) are also shown

and the lowermost part of the Pamplona Formation. These data are consistent with the age of the Sabiñanigo Sandstone (laterally equivalent to the Urroz Formation) and the base of the Pamplona Formation established from magnetobiostratigraphic data in the eastern part of the basin (Oms et al., 2003; Vinyoles et al., 2021).

The Berdún section (base: 42° 36′ 7.42″ N, 0° 52′ 19.88″ W; top: 42° 33′ 55.59″ N, 0° 53′ 33.92″ W) was sampled across the Aragón valley, between the villages of Berdún and Martes. The section begins about 1.5 km south of the eastern continuation of the Leire thrust, where two open folds (a syncline to the North and an anticline to the South) crop out (Fig. 3). The sampled section shows a rather constant SSW dip of about 20-30º in the north that slightly increases to ~ 40° in the south. From the structural point of view, sampling sites are distributed into two subgroups across the northern limb of the syncline in the north and the hinge zone and southern limb of the anticline in the south (Fig. 3). These two sampling areas are separated by an intermediate North-dipping limb that is covered by fluvial quaternary units that prevented sampling for AMS analysis. In total, 208 sites were sampled distributed along the 2000 m of the succession, which encompass the uppermost 60 m of the Larrés Formation and the complete Urroz (100 m) and Pamplona (1800 m) formations (Fig. 3). A Early-Middle Bartonian to Middle Priabonian (e.g., 40.5–36 Ma) age can be established for the succession from available biostratigraphic (Gonzalvo, 1992 and 1997) and magnetobiostratigraphic data (Hogan & Burbank, 1996; Oms et al., 2003; Costa et al., 2010; Kodama et al., 2010; Rodríguez-Pintó et al., 2012; Vinyoles et al., 2021). Considering that they partially overlap, the Izaga and Berdún sections span a total of 2800 m of sedimentary succession and record 6 Myr of the tectonic and sedimentary evolution of the Jaca-Pamplona basin.

Structural data from the sampled stratigraphic profiles have been considered for the construction of two geological cross-sections that run perpendicularly to the main structures and are based on the 1:50,000 geological maps available for the study area (del Valle de Lersundi et al., 1974; Puigdefábregas et al., 1974; Robador Moreno et al., 2024) and own observations. The western geological cross-section is ~ 10 km-long and extends from the hanging-wall of the Illón thrust to the hinge zone of the Izaga syncline, whereas the eastern geological cross-section is 15 km-long and runs from the hanging wall of the Leire thrust in the north to the hinge zone of the western Guarga syncline in the south (see locations in Fig. 3). Geological cross-sections have been built using the software Move (Petroleum Experts), which was also used for the along-strike projection of AMS data on section traces.

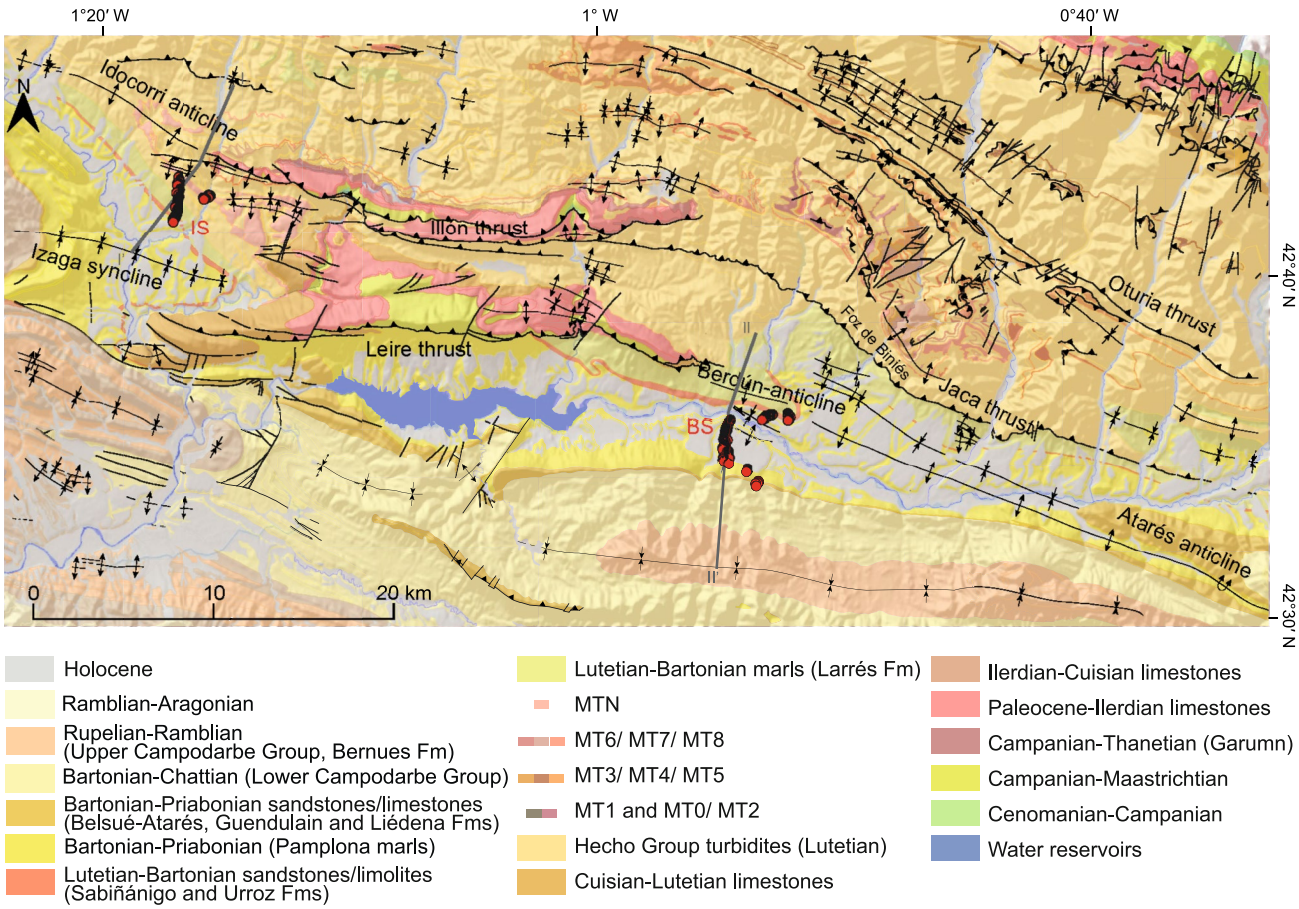

Fig. 3 Geological map around the study area (modified from Robador Moreno et al., 2024; IDENA NAVARRA visor, 2024) showing the main structures, the sampled sites (red dots) and the performed geological cross-sections (black lines)

3.2 Magnetic fabrics and magnetic mineralogy

In both sections, two to three oriented mudrock samples were collected at every site using a portable electrical power drill cooled by water. Cores were oriented in situ with an adapted magnetic compass. After sampling, the samples were cut into cylindrical standard specimens. A total of 651 specimens were measured for AMS using the KLY-3S Kappabridge (AGICO, Czech Republic), available in the Magnetic Fabrics Laboratory at the University of Zaragoza (GEOtransfer Research Group), with an applied field of 423 A/m and a frequency of 875 Hz. Average orientation of AMS axes was calculated using the Jelinek statistics (Jelínek, 1978) by means of the Anisoft 5.1.01 software (Chadima et al., 2018). The software represents the k_{max}, k_{int}, k_{min} axes orientations and magnitudes of the magnetic ellipsoid defining the magnetic fabric whose magnetic lineation is defined by k_{max} whereas the magnetic foliation is the plane perpendicular to k_{min}. The ratio of the resulting axes magnitudes, the mean susceptibility (Km), the corrected degree of anisotropy (P′) and the shape parameter (T) were all calculated. The corrected degree of anisotropy (′′) indicates the intensity of the preferred orientation of the magnetic minerals, and the shape parameter (T) indicates the shape of the ellipsoid, $-1 < T < 0$ prolate; $0 < T < +1$ oblate (Jelinek, 1981).

Other parameters of interest are the angle between the k_{min} axes and the pole of bedding and the angle between the k_{max} and the strike of the bedding which were calculated for individual samples. Angles between k_{min} axes and the pole of bedding close to zero are in agreement with bedding-parallel magnetic foliations (Type I and IIa fabrics, in terms of Parés, 2015) whereas angles above 20° can indicate an incipient cleavage overprint on magnetic fabrics and a progressive shift of magnetic foliation from a bedding-parallel to a girdle (Type IIb magnetic fabrics) or cleavage-parallel (Type III) distribution. Low angles between k_{max} and the strike of the bedding are expected in Type I and IIa fabrics (sensu Parés, 2015), whereas larger angles can indicate magnetic fabrics associated to a more intense deformation.

The evolution of the different parameters (Km, magnetic axes orientation, P′, T and angle between k_{min} and the pole of

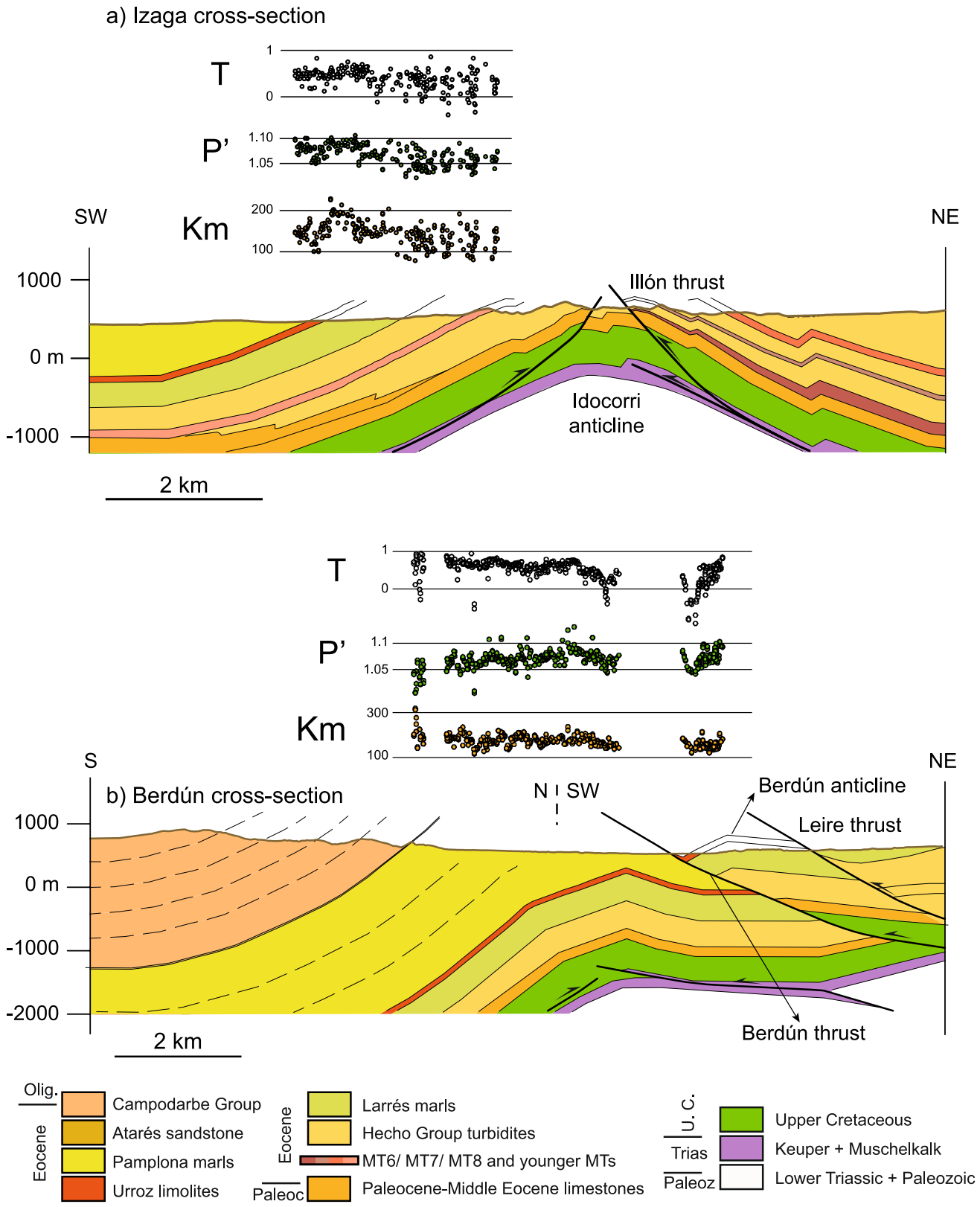

Fig. 4 Geological cross-sections of the studied sections (see locations in Fig. 3). displaying the bulk susceptibility (km), corrected degree of anisotropy (P′) and shape parameter (T). **a** Izaga section. **b** Berdún section

bedding) was analysed along the two studied sections aiming at observing changes in the evolution of the AMS related to thrusting along the different cover or basement systems. In most cases two specimens per site were analysed, although in some sites only a specimen could be analysed. Due to the high number of data and their potential scattering, running averages for the selected parameters were also calculated to reduce local noise and better visualize the data. To calculate the running averages four sites below and four sites above the target site were considered.

In order to identify the mineralogy of the studied mudstones, X-ray diffraction analyses of selected samples representative for the different formations (Hecho Group, Larrés, Urroz and Pamplona formations) were carried out using a Bruker D8 Advance ECO, following standard procedures, at the Universidad Pública de Navarra. Also, to identify magnetic mineralogy thermomagnetic runs were measured with a KLY-3 at the Magnetic Fabrics Laboratory of the Universidad de Zaragoza and with a MFK-1 at the Gams Paleomagnetic laboratory of the Montanuniversität of Leoben, Austria.

4 Results

4.1 Structural geology

As previously introduced, the study area is affected by two main ~ E–W-striking and south-directed thrust structures: the Illón thrust in the north and the Leire thrust in the south (Fig. 3). Available geological maps (del Valle de Lersundi et al., 1974; Puigdefábregas et al., 1974; Puigdefábregas, 1975; Robador Moreno et al., 2024; IDENA NAVARRA visor, 2024) reveal that these two structures show along-strike geometrical and strike changes. In map view, the central and eastern portion of the Illón structure consists of three and two outcropping south-directed thrust surfaces, respectively. Further to the East, the two outcropping thrusts change strike to NW–SE, with the northern fault laterally connecting to the folds in the Foz de Biniés area (see location in Fig. 3) and the southern fault juxtaposing the Hecho Group turbidites on top of Lutetian-Bartonian marls along the Jaca thrust and its eastern continuation along the Yebra anticline (Fig. 3). To the west, the south-directed faults forming the Illón structure branch into a single south-directed thrust that relates to a north-directed back-thrust in its footwall. This thrust-back-thrust pair is folded by the Idocorri anticline that continues laterally to the West of the lateral termination of the Illón thrust (García-Sansegundo & Barnolas, 2000). The Illón thrust is fossilized by Late Lutetian deposits accumulated in a marine carbonate platform setting simultaneously to the deposition of the Hecho Group turbidites further north and south, which attest to a major period of thrusting and uplift of the Illón structure during Middle-Lutetian times (García-Sansegundo & Barnolas, 2000). The whole structure is folded by the Idocorri anticline that formed from Late Lutetian to Oligocene times (García-Sansegundo & Barnolas, 2000). Timing of this fold affecting earlier thrusts is constrained by (i) the progressive thinning of Late Lutetian units towards its hinge zone, (ii) the geometry of the middle and upper parts of the Hecho Group, with turbidite deposits and megabreccias progressively onlapping the Late Cretaceous to Paleocene platform sequence at the hanging-wall of the Illón thrust (del Valle de Lersundi et al., 1974; Puigdefábregas et al., 1974) and (iii) the Oligocene progressive unconformity recorded at the Peña de Izaga area, westwards of the study area (see location in Fig. 3; García-Sansegundo & Barnolas, 2000).

To the south, the Leire structure is defined by a main, south-directed, outcropping thrust whose hanging-wall is deformed by one to three anticlines. These anticlines show variable wavelengths and relay laterally whereas the main south-directed thrust splays into two thrust surfaces towards both, the eastern and western terminations of the structure. Activity of the Leire thrust extended well into the Bartonian, as can be deduced from the geometrical relationships observed between the western termination of the thrust and the overlying marls of the Urroz and the lower Pamplona formations. In this western termination, the Hecho Group turbidites and the Larrés marls progressively thin to the south and finally pinch-out at the hanging-wall anticline, marking the southern limit of the Leire thrust structure, where the Urroz Formation lies on top of Lutetian limestones deposited in a shallow carbonate platform setting (Puigdefábregas, 1975). The Leire structure can be followed to the east along the Berdún and the Atarés anticlines. Development of the Illón and Leire thrust systems was partly contemporaneous with the formation of a regional cleavage domain, which intersects both structures with an oblique angle and is more penetrative in the vicinity (< 1 km) of the thrust surfaces (Labaume et al., 1985; Izquierdo-Llavall et al., 2013; Boiron et al., 2020; Saur et al., 2020; Gracia-Puzo et al., 2021).

Constructed geological cross-sections (Fig. 4a, b) show thrust geometries across the western termination of the Illón thrust (Izaga geological cross-section) and the eastern termination of the Leire thrust (Berdún geological cross-section). The Izaga section traverses the thrust-back-thrust pair forming the western segment of the Illón structure (Fig. 4a). Both the thrust and back-thrust involve Late Cretaceous and Paleocene-Eocene carbonates in their hangingwalls and are interpreted to detach (at least partly) along the Late-Middle Triassic evaporites underlying the Mesozoic rocks. The Hecho Group turbidites and megabreccia in the hanging wall of the Illón thrust are dominantly North-dipping and thin progressively towards the fault plane. Units in the footwall of the Illón thrust describe a syncline (Izaga syncline)

cored by the Pamplona marls across the section trace. In the northern limb of this syncline, the whole stratigraphic sequence shows a roughly constant dip towards the south, being affected by minor folds only in the area located at a distance of ≤ 1 km from the back-thrust. Globally, the geometry of the Illón structure and the Izaga syncline impose an antiformal geometry of the underlying Mesozoic sequence (Idocorri anticline). The absence of a thick Late-Middle Triassic detachment in neighbouring wells (i.e., the Roncal well; Lanaja, 1987) and the presence of short-wavelength gravity highs in the area (Toro et al., 2021) suggest that the Mesozoic antiform relates at depth to a basement anticline.

To the East, the Berdún geological cross-section traverses the eastern termination of the Leire structure (Fig. 4b). At the geological cross-section trace, the Leire thrust juxtaposes Lutetian-Bartonian on top of Bartonian-Priabonian marls (Pamplona Fm). Its footwall is characterized by a dominantly South-dipping sequence defining the northern limb of the Guarga syncline (cored by the Campodarbe Group at the section trace). Geological maps in the sampled area suggest that the northernmost outcrops in the northern limb of the Guarga syncline are affected by a series of open folds (including the Berdún anticline, Fig. 3). These folds would laterally accommodate part of the shortening of the Leire main thrust cropping out further west. Geological map (Fig. 3) reveals two main NW–SE-trending anticlines (sampled for AMS in this study) cored by the Larrés (northern anticline) and Pamplona marls (southern anticline). Position of mapped stratigraphic contacts and bedding dips measured in the field require the presence of a south-directed thrust separating the two anticlines (hereinafter the Berdún thrust, Fig. 4b). This thrust is hardly recognized in the field due to the similar lithology of stratigraphic units in both its hanging and footwall, but mapping criteria strongly impose the presence of this undetected structure that was not reported in previously published geological maps across the area. The overall geometry of the marly units traversed by the Berdún geological cross-section reveals a general antiformal geometry, the hinge zone of the antiform being centred at the Leire thrust area. Similarly to the Izaga geological cross-section, a main basement anticline has been interpreted at depth to explain the antiform described by cover units.

4.2 Magnetic fabrics

4.2.1 Magnetic mineralogy and bulk scalar parameters

XRD results indicate that the studied Eocene mudrocks of the Jaca-Pamplona basin are made up mainly of diamagnetic minerals such as calcite and quartz, and by paramagnetic phyllosilicates such as chlorite and illite-muscovite (Fig. 5a) in consistency with other studies carried out in the area (Izquierdo-Llavall et al., 2013; Boiron et al., 2020) Moreover, Saur et al. (2020) with X-ray computed tomography techniques have described the organization of the quartz and calcite grains at different stages of deformation.

Carbonate contents range between 33.4 and 53.5 wt% and can be associated with biological productivity. Quartz and clay mineral contents range between 23–31.8 wt% and 19.4–34.8 wt%, respectively, and represent the detrital fraction of the studied marls. Thermomagnetic runs show similar behavior. Curves are not reversible; the heating curves have a flat-concave shape until 400–450 °C where the susceptibility increases and decay at 580 °C related to the presence of magnetite. The cooling curves show a large increase of susceptibility at around 580 °C indicating the neoformation of magnetite (Fig. 5b). In consonance with their composition, the bulk susceptibility (km) analysed in the mudrocks of both sections ranges from 75×10^{-6} to 317×10^{-6} S.I., with an average of 155×10^{-6} S.I. (Fig. 6a). The corrected degree of anisotropy (P') in both sections ranges from 1.006 to 1.13, with an average of 1.068 (Fig. 6b). The shape parameter (T) in both sections is generally homogeneous and oblate ellipsoids dominate (Fig. 6c).

4.2.2 Scalar parameters vs. stratigraphic sections

Analysing the data along the stratigraphic sequences (Fig. 7) allows observing some patterns. The bulk susceptibility (km) curve shows changes or inflection points that coincide with changes in the lithostratigraphic formations, suggesting that it is primarily influenced by lithology (Fig. 7a). Furthermore, there is a slight general trend, from bottom to top, to higher susceptibility values. The susceptibility (Fig. 7a) is slightly lower (average of 121×10^{-6} S.I.) in the lowermost 450 m of the Izaga section (Hecho Group) if compared to the rest of the succession (Larrés, Urroz and Pamplona formations) (average of 153×10^{-6} S.I.). In the Izaga section, the general trend of the Km increases from the meter 450 m to meter 900 m, where there is a maximum and then decreases during the next 100 m. In the uppermost 100 m of the section, the values increase slightly and then remain constant. Comparable values are found throughout the Berdún section (average of 168×10^{-6} S.I.). Several increase–decrease cycles can be observed over a background of broadly constant values (Fig. 7a).

The corrected degree of anisotropy (P′) in the Izaga section increases from the meter 450 to the meter 900 of the sampled sequence (i.e., from North to South in map view), therefore is likely to be, at least partially, conditioned by mineralogy, whereas in the Berdún section slightly decreases towards the top, defining the curve a well-marked peak at its base (decreasing/increasing cycle) (Fig. 7b). The shape parameter (T) in the first 650 m of the Izaga section indicates mainly an oblate to triaxial ellipsoid despite its high dispersion. In the upper half of the section, it becomes more

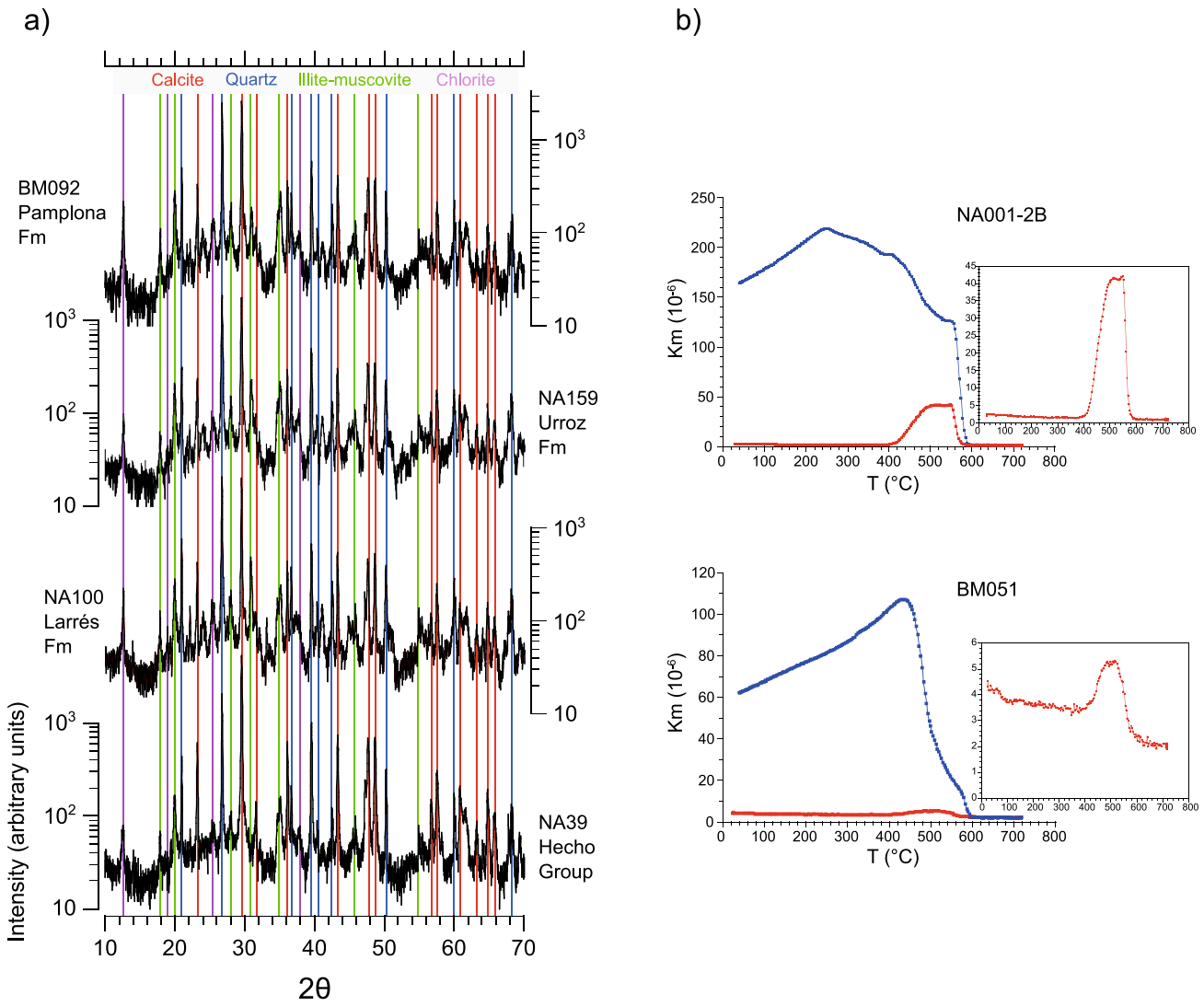

Fig. 5 **a** Position-sensitive-detector X-ray diffraction (PSD-XRD) patterns of selected mudrock samples from the different stratigraphic units included in the studied successions. **b** Representative thermomagnetic runs of the studied sections

grouped and oblate. In the Berdún section, the lowermost 450 m display a conspicuous change in the shape of the ellipsoids. The ellipsoids undergo a progressive decrease in the T parameter, beginning with an oblate ellipsoid that undergoes a transition first to a triaxial ellipsoid and subsequently to a prolate ellipsoid. The ellipsoid then returns to an oblate shape with T values greater than 0.5. Around the meter 900 there is a slightly variation and the ellipsoids become less oblate. At about meter 1800 there is a short interval with prolate and triaxial ellipsoids (Fig. 7c). Those variations do not seem to coincide with a lithological change.

4.2.3 Magnetic fabrics types

The orientation of the axes of the magnetic ellipsoid are represented before (Fig. 6d) and after bedding correction (BBC and ABC respectively) (Fig. 6e). The Izaga section shows k_{max} axes grouped ABC in a WNW-ESE horizontal direction contained in the bedding plane (Fig. 8a), with a slightly increase in the angle between them towards the top of the section (Fig. 7e), parallel to the Pyrenean direction and to folds and thrusts in the area. K_{min} axes are perpendicular to bedding and therefore subvertical ABC, thus the magnetic foliation is parallel to the bedding (in general less than 10° of difference) (Fig. 7d) and correspond with a Type IIa fabric (Fig. 8a–c). The Berdún section also shows a roughly NW–SE direction of k_{max} axis parallel to bedding and to the Pyrenean structural direction, except for the 250–600 m interval (Fig. 7e), but with a slightly higher dispersion that the Izaga section (Fig. 8d). The k_{max}-So angle decreases gradually in the following meters. However, k_{min}-So relationship shows two different behaviours in the

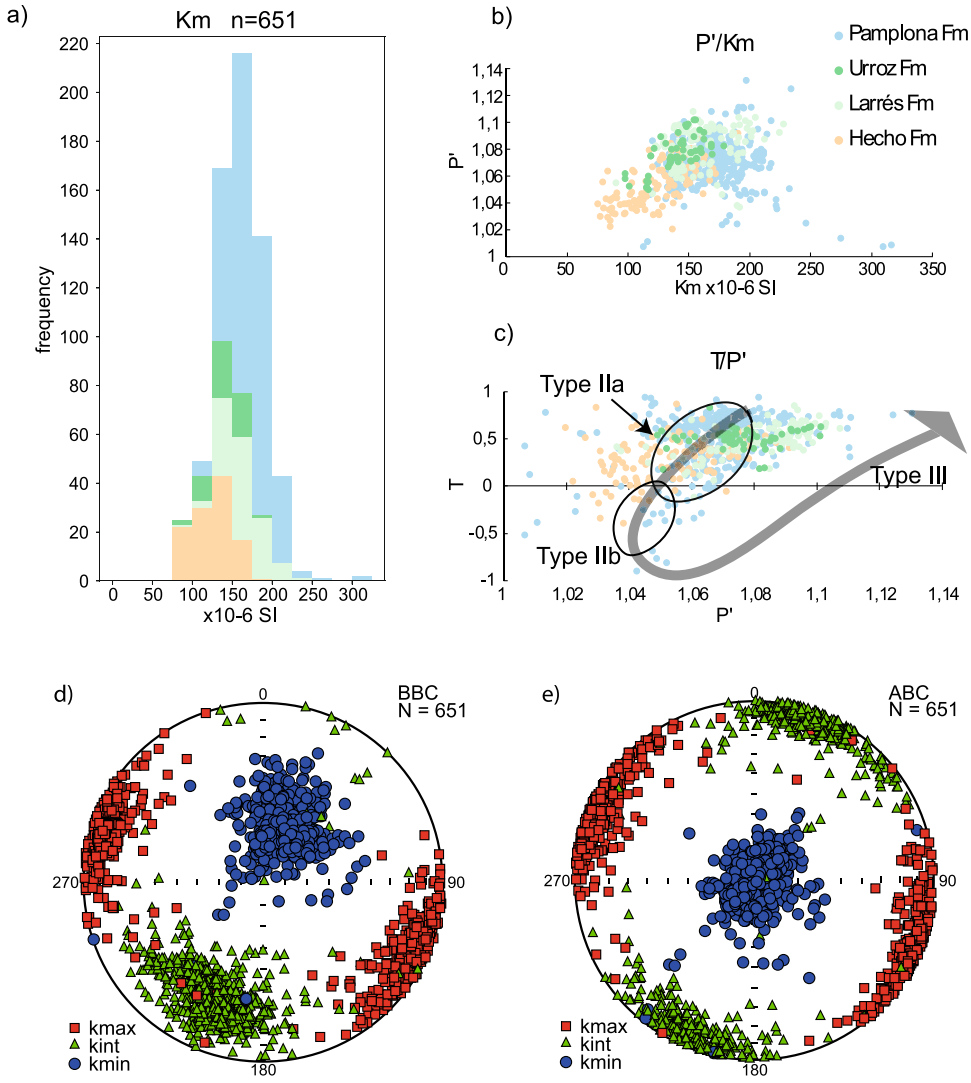

Fig. 6 Scalar parameters and directional distribution of the magnetic fabrics measured in both sections. **a** Bulk susceptibility (km) histogram. **b** Corrected degree of anisotropy (P′) versus bulk susceptibility. **c** Shape parameter (T) and corrected degree of anisotropy (P′) diagram. T/P′ diagram with the type of magnetic fabrics and evolution of the parameters with strain (modified from Parés, 2004). **d** Equal area projection of the magnetic ellipsoid of the total measured specimens before bedding correction (BBC). **e** Equal area projection of the magnetic ellipsoid of the total measured specimens after bedding correction (ABC)

Berdún section. Although the k_{min} remain subparallel to the pole of the bedding plane (i.e. magnetic foliation parallel to bedding) with differences between them lower than 10°–15° for most of the measured specimens (Fig. 7d), an incipient gridle perpendicular to k_{max} appears (Fig. 8e), corresponding to a transition (or a mixing) between Type IIa and Type IIb fabric (note that higher values of the k_{min}-So pole angle and k_{max}-So angle correspond with prolate samples, Fig. 7c). On the other hand, the upper half of the section show k_{min} axes perpendicular to bedding (Fig. 8f), defining a Type IIa fabric. In the Type IIa fabric, short axes of quartz and calcite grains are concentrating around the pole of the bedding whereas in the Type IIb fabric the concentration of the quartz grains remains around the pole of the bedding and the calcite grains are concentrate around the k_{min} axes. In both types the long axes of the quartz and calcite grains are displayed parallel to k_{max} axes (Saur et al., 2020).

The shape parameter (T) and the axes orientation of the magnetic ellipsoid do not appear to be related to lithological changes. These parameters show variations in the same interval (0–450 m) and, to a lesser extent, around meter 1800 in the Berdún section (Fig. 7c, d). These behaviours have been observed by other authors in Eocene marls in the South Pyrenean Zone being related to different stages of LPS, folding and thrusting (Larrasoaña et al., 1997, 2004; Mochales et al., 2010; Pueyo Anchuela et al., 2010; Boiron et al., 2020; Gracia-Puzo et al., 2021; Menzer et al., 2024).

5 Discussion

5.1 Significance of magnetic fabrics in the studied mudrocks

XRD results indicate that the studied Eocene mudrocks of the Jaca-Pamplona basin are made up mainly by biogenic (carbonates) and detrital (quartz and phyllosilicates such as chlorite and illite-muscovite) minerals (Fig. 5a). The bulk

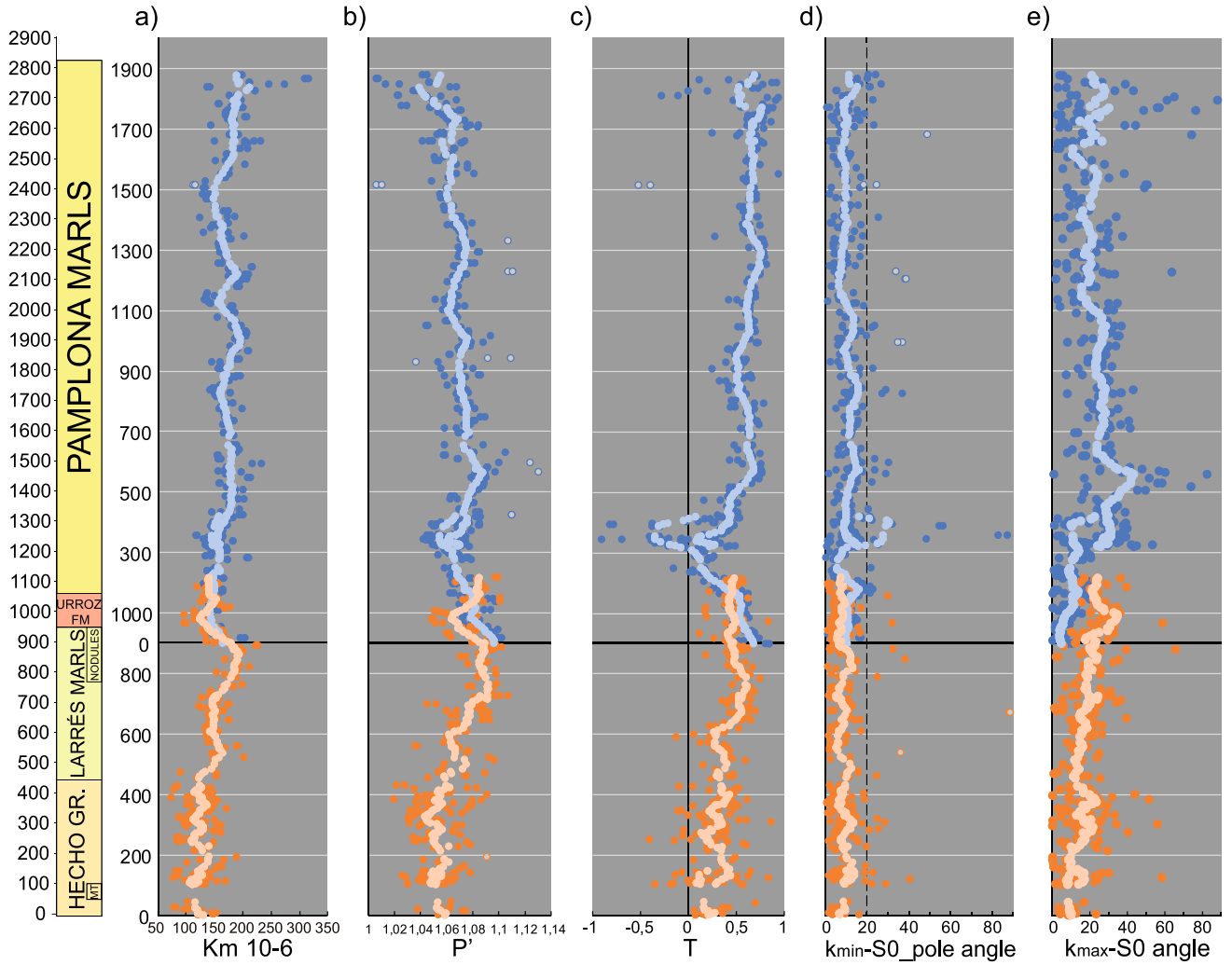

Fig. 7 Scalar parameters versus sedimentary pile of both sections (in orange Izaga section; in blue Berdún section). Running averages are in soft colours, grey dots are considered outliers and are not used to calculate the running averages. **a** Bulk susceptibility (km). **b** Corrected degree of anisotropy (P′). **c** Shape parameter (T). **d** Angle between k_{min} and the pole of the bedding. **e** Angle between k_{max} and the bedding

susceptibility (km) analysed in both sections ranges from 75×10^{-6} to 317×10^{-6} S.I. (Fig. 6a), with an average of 155×10^{-6} S.I. This attests for the mixture of diamagnetic (carbonates and quartz) and paramagnetic (chlorite and illite-muscovite) minerals, with a subdued contribution of ferrimagnetic minerals (e.g., magnetite, Fig. 5b), that typifies most marly sedimentary successions (Rochette, 1987). These results indicate that the AMS signal of the studied Eocene mudrocks can be interpreted in terms of the preferential orientation of paramagnetic phyllosilicates, as has been further demonstrated by previous rock-magnetic and mineralogical data obtained for the studied sequences (e.g., Larrasoaña et al., 2004; Pueyo-Anchuela et al., 2012b, 2013; Pocoví et al., 2014).

The magnetic fabrics of all the studied samples correspond with those that signal the imprint of initial compression reported typically for weakly deformed mudrocks (Tarling & Hrouda, 1993; Parés et al., 1999). Thus, most samples display Type IIa fabrics in which k_{max} axes cluster perpendicularly to the shortening direction, albeit with a large dispersion within the bedding plane, at the same time that k_{min} axes remain perpendicular to bedding (Fig. 8a, d). This type of oblate fabric ($T > 0.25$) is observed throughout the Izaga (although in the first 650 m there also triaxial ellipsoids) and the middle and upper part of the Berdún sections (Figs. 7c, 8a–c, f), and has been typically associated to syn-sedimentary LPS (Parés et al., 1999; Larrasoaña et al., 2004; Parés, 2015; Menzer et al., 2024). In the lower part (< 450 m) of the Berdún section, Type IIb fabrics (characterized by k_{min} axes displaying a girdle that is parallel to the shortening direction and perpendicular to the clustering of k_{max} axes, Fig. 8e) are observed. They relate

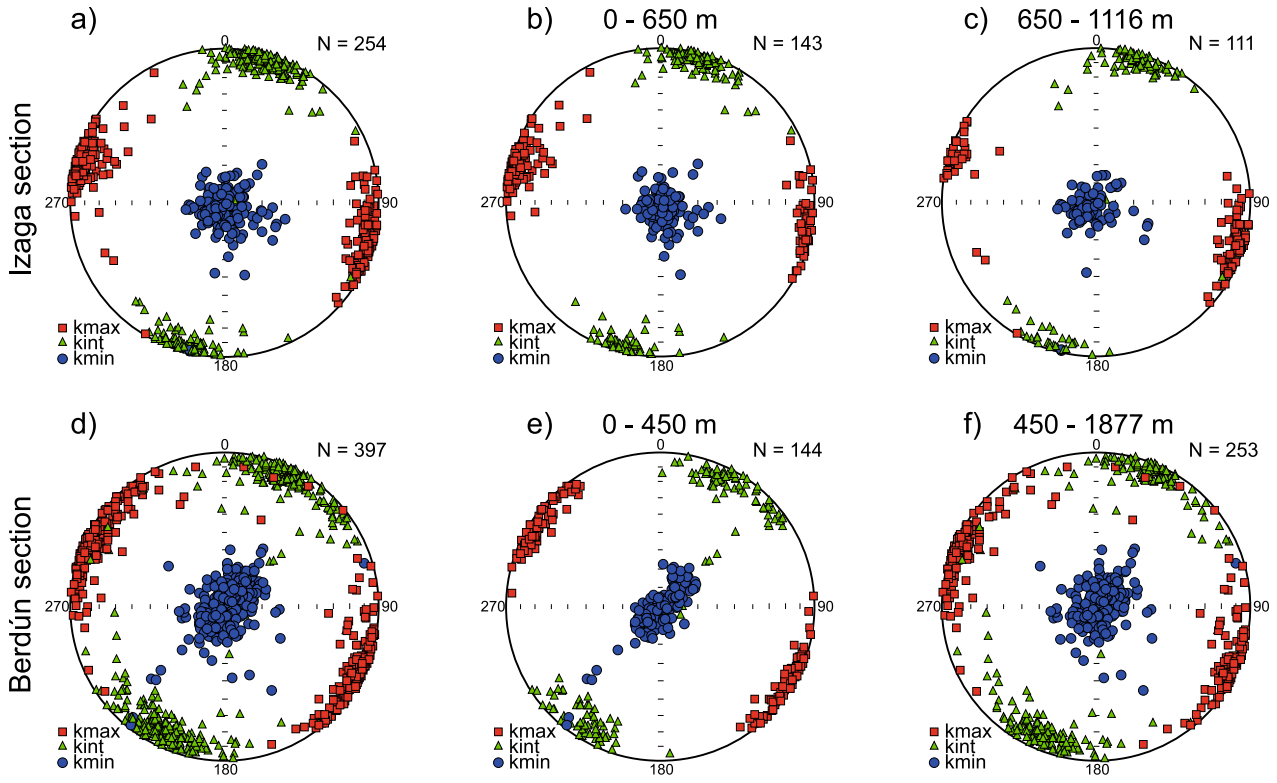

Fig. 8 Equal area projection after bedding correction (ABC) of the magnetic fabrics of the studied sections. **a** Complete Izaga section. **b** Lowermost 650 m of the Izaga section. **c** Upper half of the Izaga section. **d** Complete Berdún section. **e** Basal 450 m of the Berdún section. **f** Upper 1427 m (450–1877 m) of the Berdún section

with a moderate decrease of P' and a pronounced decrease of T (that approaches zero or becomes negative, Fig. 7b, c). This type of fabric has been associated either with the effect of a more intense LPS (Parés et al., 1999; Larrasoaña et al., 2004; Parés, 2004, 2015, Soto et al., 2009) or the later imprint of shearing and cleavage development in the vicinity of thrust surfaces (Hirt et al., 2004; Boiron et al., 2020; Gracia-Puzo et al., 2021; Menzer et al., 2024). In contrast to Boiron et al. (2020) and Gracia-Puzo et al. (2021), whose studies were carried out in areas very close to the Berdún section, magnetic fabrics associated to a higher deformation were not identified in this study. This difference is due to the different structural position relative to the Leire thrust. In this study, samples with a more distant (and consequently less affected) position with respect to the thrust surface have been considered compared to those in Boiron et al. (2020) and Gracia-Puzo et al. (2021). In order to evaluate the potential influence of LPS versus thrust-related shearing in our samples, we have analyzed their magnetic fabrics in the context of their structural position along the newly constructed geological cross-sections (Fig. 4a, b).

For the Berdún section, Type IIa fabrics signaling the initial effect of LPS are reported throughout the uppermost 1400 m, which are located ~ 1 to 4 km away from the trace of the previously undetected thrust identified in the marly sequence of the Leire footwall (the Berdún thrust, Fig. 4b). Conversely, Type IIb fabrics are found in the lowermost 450 m of the succession, in samples located at a distance of less than 1 km away to the north and south of the Berdún thrust (Fig. 4b). These results strongly suggest that these Type IIb fabrics have been affected by shearing associated to the emplacement of the thrust; in absence of visible thrust-related cleavage, we interpret that gradual decrease of the k_{max}-So angle attests to the vicinity of the thrust surface. Reported AMS data are in full agreement with the results presented by Boiron et al. (2020) and Gracia-Puzo et al. (2021) in the central segment of the Leire thrust and by Menzer et al. (2024) near the Oturia thrust in the eastern part of the Jaca-Pamplona basin, where mudrock fabrics affected by shearing were reported at a distance of < 1 km away from thrust surfaces.

Apart from a consistency with previous AMS results in the area, it is noticeable that magnetic fabrics observed in the Berdún section provide not only an indirect confirmation for the presence of the newly identified Berdún thrust, as deduced from the construction of the geological cross-section, but also enable to infer a NW–SE orientation for this previously undetectedthrust that is slightly oblique to

the shortening direction as deduced from the orientation of the magnetic ellipsoids from the rest of the section. This NW–SE thrust strike is consistent with the trend of the Berdún anticline in its hangingwall, as well as with the trend of the Illón thrust to the north of the section trace (Fig. 3). It is also important to highlight the fact that, incidentally, these results also suggest that the studied magnetostratigraphic sequence is not complete (see Fig. 4b); according to the geological cross-section, a missing interval at the base of the Pamplona Formation is expected, with the implications it might have for interpreting the magnetobiostratigraphic results of the Berdún section in future studies.

The interpretation in the Izaga section is more straightforward given the fact that all the studied samples display Type IIa fabrics and are located between ~ 3 and 8 km south of the Illón thrust. Keeping in mind the results by Hirt et al., (2004), Boiron et al., (2020), Gracia-Puzo et al., (2021) and Menzer et al., (2024), as well as our own data from the Berdún section, this clearly points to LPS, and not to shearing along the thrust surface, as the underlying mechanism that caused the observed fabrics. Yet, two distinct groups of samples among Type IIa fabrics can be distinguished along the section: triaxial to oblate ellipsoids with high dispersion samples, identified in the lowermost 650 m of the section, and samples with oblate ellipsoids (mean T values above 0.25) observed higher up in the section (Fig. 4a). The fact that this shift does not mimic the increase in susceptibility values observed at about meter 450 suggests that changes in the concentration of phyllosilicates are not responsible for the change in the shape of the magnetic ellipsoids. We interpret that the shift from triaxial to oblate ellipsoids observed at about meter 650 signals a less developed magnetic lineation in response to a decrease in the strain associated to LPS.

5.2 Tectonic evolution of the Southern Pyrenees

The temporal span covered by the Izaga and Berdún sections begins at the latest Lutetian (ca. 42 Ma, base of the Izaga section) (Payros et al., 1999), and finishes in the Middle Priabonian, when the marine-continental transition takes place in the Jaca-Pamplona basin (ca. 36 Ma, top of the Berdún section) (Garcés et al., 2020). AMS results presented here have been linked to two main types of deformation, LPS versus thrust-related shearing, and might therefore help to unravel the tectonic evolution of a part of Pyrenean range where information on the activity of different thrust systems have yielded somehow ambiguous ages (see discussions in Séguret, 1972; Fernández et al., 2012; Muñoz et al., 2013, 2018; Labaume et al., 2016b) (Fig. 2).

The Illón thrust, located north of the Izaga section, was mainly active up to the Middle Lutetian, with later deformation being likely restricted to folding from the Late Lutetian to the Early Oligocene (Idocorri anticline, García-Sansegundo & Barnolas, 2000). Since sediments of the Izaga section accumulated between the latest Lutetian (ca. 42 Ma) and the Middle Bartonian (ca. 40 Ma), the LPS recorded by its mudrock fabrics has to be related to the strain associated to other thrust units located further north. The western prolongation of the Oturia thrust is considered an unlikely possibility, given its emplacement and main activity between the Late Bartonian and the Priabonian (Labaume et al., 2016b; Menzer et al., 2024), unless an important W-E diachroneity is involved in the development of the structure. The most likely candidate for the LPS recorded by the Izaga section is the Larra thrust system, which developed synchronously with the deposition of the Izaga section sequence before becoming inactive, likely during the Late Bartonian (Labaume et al., 2016b). With these caveats in mind, we interpret that the shift observed between the prolate and oblate Type IIa fabrics in the Izaga section is recording the decrease in the activity of the distant Larra thrust system, which seems to validate the chronology proposed by Labaume et al. (2016b).

For interpreting the magnetic fabrics of the Berdún section it is necessary to first consider the Type IIb fabrics reported in the lower part of the succession, since they have been overprinted by shear along the previously undetectedthrust identified in the geological cross-section (i.e., the Berdún thrust). This thrust must have post-dated deposition of, at least, the lower third part of the Pamplona Formation (e.g. Early Priabonian), but its activity occurred or continued most likely between the Late Priabonian and the Rupelian (Early Oligocene) as deduced from tecto-sedimentary relationships reported for the eastern continuation of the Leire thrust in the Atarés anticline (Montes, 2009). The rest of the Berdún section, characterized by Type IIa fabrics, is recording strain related to syn-sedimentary LPS, for which three main alternative structures emerge: (1) the Leire thrust itself, likely active from Lutetian-Bartonian (Sect. 4.1) and between Priabonian and Rupelian times; (2) the Gavarnie thrust and its splay into the cover, the Oturia thrust, whose activity begun after cessation of the Larra thrust system during the latest Bartonian and extended beyond the Priabonian (Labaume et al., 2016b; Menzer et al., 2024) and (3) the basement thrusts identified in the study area at an intermediate position between the Gavarnie and the Guarga thrusts (Toro et al., 2020). Regarding (2), results from the footwall of the Oturia thrust have shown that Type IIa fabrics are observed at distances very close to the thrust as long as they have not been obliterated by shear along the thrust surface (e.g. > 1 km; absent macroscopic cleavage) (Menzer et al., 2024). Furthermore, results from the western (Soto et al., 2009) and eastern (Parés et al., 1999) parts of the Ebro foreland basin have shown that Type IIa fabrics can be observed to distances up to 30–50 km away from the Pyrenean deformation front. Hence, it seems that distinguishing between

a far- and a near-field effect of thrust-induced LPS is virtually impossible given the fact that magnetic fabrics seem to detect very subtle strain conditions, and that no further changes are observed till the fabrics become obliterated by additional strain imposed by shear in the vicinity of thrust surfaces.

A final aspect that deserves attention is the fact that an interval of triaxial ($T = \sim 0$) and prolate ($T < -0.25$) ellipsoids are observed in the uppermost part of the studied sequence. It is defined in the uppermost part of the Pamplona Formation, just below the Atarés Sandstone that signals the rapid continentalization of the Jaca-Pamplona basin. Such continentalization has been linked to a base level drop in the basin driven likely by the combination of enhanced tectonic uplift and a sea level fall (Costa et al., 2010; Payros et al., 2000). We interpret that the triaxial and prolate ellipsoids in the topmost marine marls indicate the imprint of LPS-related strain conditions, which we tentatively link to enhanced thrust activity to the north of the section (likely the Gavarnie thrust) in what might be, to our knowledge, the first direct evidence for the major role of tectonics in driving the continentalization of the South Pyrenean basin.

6 Conclusions

An analysis of magnetic fabrics along two magnetostratigraphic sections, Izaga and Berdún (2800 m in total) spanning from Late Lutetian to Middle Priabonian, has been carried out in the central Jaca-Pamplona basin. This detailed analysis allows us to know the temporal and spatial evolution of the deformation recorded by the magnetic fabrics. The AMS signal of the studied mudrocks can be interpreted in terms of the preferential orientation and deformation of paramagnetic phyllosilicates.

In the Izaga section, two different types of magnetic fabrics have been identified. In the lowermost 650 m of the section, Type IIa fabrics with triaxial ellipsoids were identified, while Type IIa fabrics with oblate ellipsoids were found in the upper half of the section. Those fabrics are associated with a decrease in deformation (from triaxial to oblate) driven by layer parallel shortening (LPS) and can be related with a reduction in the activity of the Larra thrust system.

In the Berdún section two types of the magnetic fabrics have been identified. Type IIb fabrics are found in the basal 450 m and Type IIa fabrics appear in the upper 1400 m of the section. The Type IIa fabrics are related to LPS, but it is not possible to determine to which structure it would be associated. The Type IIb fabrics have been affected by shearing and allow us to corroborate the presence of a previously undetected thrust in this part of the section which must correspond to the lateral expression of the Berdún thrust. Finally, the upper section of the Pamplona Formation in the Berdún section shows prolate magnetic fabrics that can be related to an enhance of the tectonic activity that could have led to the continentalization of the basin.

7 Supplementary data

Supplementary data available in: https://doi.org/10.5281/zenodo.11221312.

Acknowledgements The authors thank Gilen Bernaola and Marcos Marcén for their help during field work, and Francho Gracia-Puzo for the help in the discussion of the results. This study was funded by project UKRIA-4D (PID2019-104693GB-I00) of the Spanish Ministry of Science and Innovation, "ERDF A way of making Europe", which also covered the predoctoral contract of Pablo Sierra-Campos (PRE2020-092425). Pablo Calvín acknowledges funding from FJC2019-041058-I (Ministerio de Ciencia e Innovación Spain) contract. We acknowledge the two anonymous reviewers for their positive and constructive comments, and also Sameer Ahamed for editorial handling.

Funding Open Access funding provided thanks to the CRUE-CSIC agreement with Springer Nature.

Declarations

Conflict of interest The authors declare no competing interests.

References

Abd Elmola, A., Buatier, M., Monie, P., Labaume, P., Trap, P., & Charpentier, D. (2018). 40Ar/39Ar muscovite dating of thrust activity: a case study from the Axial Zone of the Pyrenees. *Tectonophysics, 745*, 412–429. https://doi.org/10.1016/j.tecto.2018.09.004

Boiron, T., Aubourg, C., Grignard, P. A., & Callot, J. P. (2020). The clay fabric of shales is a strain gauge. *Journal of Structural Geology, 138*, 104130. https://doi.org/10.1016/j.jsg.2020.104130

Borradaile, G. J. (2001). Magnetic fabrics and petrofabrics: Their orientation distributions and anisotropies. *Journal of Structural Geology, 23*(10), 1581–1596.

Borradaile, G. J., & Henry, B. (1997). Tectonic applications of magnetic susceptibility and its anisotropy. *Earth-Science Reviews, 42*(1–2), 49–93.

Borradaile, G. J., & Jackson, M. (2004). Anisotropy of magnetic susceptibility (AMS): Magnetic petrofabrics of deformed rocks. *Geological Society, London, Special Publications, 238*(1), 299–360.

Borradaile, G. J., & Jackson, M. (2010). Structural geology, petrofabrics and magnetic fabrics (AMS, AARM, AIRM). *Journal of Structural Geology, 32*(10), 1519–1551.

Caricchi, C., Cifelli, F., Kissel, C., Sagnotti, L., & Mattei, M. (2016). Distinct magnetic fabric in weakly deformed sediments from extensional basins and fold-and-thrust structures in the Northern Apennine orogenic belt (Italy). *Tectonics, 35*(2), 238–256.

Chadima, M., Hrouda, F., & Jelinek, V. (2018). *Anisotropy data browser for Windows*. Agico, Inc.

Choukroune, P. (1992). Tectonic evolution of the Pyrenees. *Annual Review of Earth and Planetary Sciences, 20*(1), 143–158.

Cifelli, F., Mattei, M., Hirt, A. M., & Günther, A. (2004). The origin of tectonic fabrics in "undeformed" clays: the early stages of deformation in extensional sedimentary basins. *Geophysical Research Letters*. https://doi.org/10.1029/2004GL019609

Costa, E., Garces, M., López-Blanco, M., Beamud, E., Gómez-Paccard, M., & Larrasoaña, J. C. (2010). Closing and continentalization of the South Pyrenean foreland basin (NE Spain): Magnetochronological constraints. *Basin Research, 22*(6), 904–917. https://doi.org/10.1111/j.1365-2117.2009.00452.x

del Valle de Lersundi, J., Puigdefábregas, C., & Sánchez Carpintero, I. (1974). Mapa geológico de la Hoja nº 143 (Navascués). Mapa Geológico de España E. 1:50.000. Segunda Serie (MAGNA), Primera edición. IGME. Depósito legal: M-6791-1978.

Fernández, O., Muñoz, J. A., Arbués, P., & Falivene, O. (2012). 3D structure and evolution of an oblique system of relaying folds: The Aínsa basin (Spanish Pyrenees). *Journal of the Geological Society, 169*(5), 545–559. https://doi.org/10.1144/0016-76492011-068

Garcés, M., López-Blanco, M., Valero, L., Beamud, E., Muñoz, J. A., Oliva-Urcia, B., Vinyoles, A., Arbués, P., Cabello, P., & Cabrera, L. (2020). Paleogeographic and sedimentary evolution of the South Pyrenean foreland basin. *Marine and Petroleum Geology, 113*, 104105. https://doi.org/10.1016/j.marpetgeo.2019.104105

García-Lasanta, C., Oliva-Urcia, B., Román-Berdiel, T., Casas, A. M., & Pérez-Lorente, F. (2013). Development of magnetic fabric in sedimentary rocks: Insights from early compactional structures. *Geophysical Journal International, 194*(1), 182–199. https://doi.org/10.1093/gji/ggt098

García-Sansegundo, J., & Barnolas, A. (2000). La terminación occidental del cabalgamiento de la Sierra de Illón (Pirineos Navarros, España). *Geo-Temas, 1*(2), 93–96.

Gonzalvo, C. (1992). Los foraminíferos planctónicos del tránsito Eoceno-Oligoceno: Bioestratigrafía y cronoestratigrafía. *Tesis doctoral Universidad de Zaragoza*, 202 pp.

Gonzalvo, C. (1997). Correlación Paleoceanográfica mediante foraminíferos planctónicos del tránsito Eoceno Medio-Eoceno Superior entre la Cordillera Bética y el Pirineo. *Revista De La Sociedad Geológica De España, 10*(1), 29–38.

Gracia-Puzo, F., Aubourg, C., & Casas-Sainz, A. (2021). A fast way to estimate the clay fabric from shale fragments. Key example from a strained thrust footwall (Pyrenees). *Journal of Structural Geology, 152*, 104443. https://doi.org/10.1016/j.jsg.2021.104443

Graham, J. W. (1954). Magnetic anisotropy, an unexploited petrofabric element. *Geological Society of America Bulletin, 65*, 1257–1258.

Hirt, A. M., Lowrie, W., Lüneburg, C., Lebit, H., & Engelder, T. (2004). Magnetic and mineral fabric development in the Ordovician Martinsburg Formation in the Central Appalachian fold and thrust belt, Pennsylvania. *Geological Society, London, Special Publications, 238*(1), 109–126. https://doi.org/10.1144/GSL.SP.2004.238.01.09

Hogan, P. J., & Burbank, D. W. (1996). Evolution of the Jaca piggyback basin and emergence of the External Sierra, southern Pyrenees. In P. F. Friend & C. J. Dabrio (Eds.), *Tertiary basins of Spain* (pp. 153–160). Cambridge Univ. Press.

IDENA NAVARRA Visor. (2024). *Mapa geológico digital continuo 1:25000, [en línea] Navarra, Gobierno de Navarra*. Información geográfica propiedad del Gobierno de Navarra. https://idena.navarra.es/navegar/#ZXh0fGJhc2V8bWFwYWJhc2V8bGF5ZXJzfHV8Ly9pZGVuYS5uYXZhcnJhLmVzL29nYy93bXN8bnxnZW9sb2dpYXxvfHZ8aHx1cnxmfHR8SURFTkF8aXxsY2F0LTEtMV4xXjYwNzYxNS4yNzV8NDcwNjU1NS4zNzZ8NjY5MDU1LjI3NXw0NzM0MzU1LjM3Nl4kMHxASXxKfEt8TF18MXwyfDN8QCQ0fDV8Nnw3fDh8SHw5fC0xfEF8LTF8QnwtNXxDfC01fER8RXxGfEddXV0=

Izquierdo Llavall, E., Calvín, P., Toro, R., Pueyo, E., Casas, A., Larrasoaña, J. C., Muñoz Ochando, I., Sierra, P., & Orera, A. (2023). *Burial and structural evolution of a deformed foreland basin: The south-western Pyrenees*. EGU General Assembly 2023, Vienna, Austria, 24–28 Apr 2023, EGU23-9217. https://doi.org/10.5194/egusphere-egu23-9217

Izquierdo-Llavall, E., Aldega, L., Cantarelli, V., Corrado, S., Gil-Peña, I., Invernizzi, C., & Casas, A. M. (2013). On the origin of cleavage in the Central Pyrenees: Structural and paleo-thermal study. *Tectonophysics, 608*, 303–318. https://doi.org/10.1016/j.tecto.2013.09.027

Jelínek, V. (1978). Statistical processing of anisotropy of magnetic susceptibility measured on groups of specimens. *Studia Geophysica Et Geodaetica, 22*(1), 50–62.

Jelinek, V. (1981). Characterization of the magnetic fabric of rocks. *Tectonophysics, 79*(3–4), T63–T67.

Jolivet, M., Labaume, P., Monié, P., Brunel, M., Arnaud, N., & Campani, M. (2007). Thermochronology constraints for the propagation sequence of the south Pyrenean basement thrust system (France-Spain). *Tectonics*. https://doi.org/10.1029/2006TC002080

Kodama, K. P., Anastasio, D. J., Newton, M. L., Parés, J. M., & Hinnov, L. A. (2010). High-resolution rock magnetic cyclostratigraphy in an Eocene flysch, Spanish Pyrenees. *Geochemistry, Geophysics, Geosystems*. https://doi.org/10.1029/2010GC003069

Labaume, P., Meresse, F., Jolivet, M., & Teixell, A. (2016a). Exhumation sequence of basement thrust units in the westcentral Pyrenees. Constraints from apatite fission track analysis. *Geogaceta, 60*, 11–14.

Labaume, P., Meresse, F., Jolivet, M., Teixell, A., & Lahfid, A. (2016b). Tectonothermal history of an exhumed thrust-sheet-top basin: An example from the south Pyrenean thrust belt. *Tectonics, 35*, 1280–1313. https://doi.org/10.1002/2016TC004192

Labaume, P., Mutti, E., Séguret, M., & Rosell, J. (1983). Mégaturbidites carbonatées du bassin turbiditique de l'Eocène inférieur et moyen sud-pyrénéen. *Bulletin De La Société Géologique De France, 7*(6), 927–941.

Labaume, P., Séguret, M., & Seyve, C. (1985). Evolution of a turbiditic foreland basin and analogy with an accretionary prism: Example of the Eocene south-Pyrenean basin. *Tectonics, 4*(7), 661–685.

Labaume, P., & Teixell, A. (2018). 3D structure of subsurface thrusts in the eastern Jaca Basin, southern Pyrenees. *Geologica Acta, 16*(4), 477–498. https://doi.org/10.1344/GeologicaActa2018.16.4.9

Lanaja, J. M. (1987). *Contribución de la exploración petrolífera al conocimiento de la geología de España*. IGME.

Larrasoaña, J. C., Pueyo, E. L., & Parés, J. M. (2004). An integrated AMS, structural, palaeo-and rock-magnetic study of Eocene marine marls from the Jaca-Pamplona basin (Pyrenees, N Spain); new insights into the timing of magnetic fabric acquisition in weakly deformed mudrocks. *Geological Society, London, Special Publications, 238*(1), 127–143.

Larrasoaña, J. C., Pueyo-Morer, E. L., Millán-Garrido, H., Parés, J. M., & Del Valle, J. (1997). Deformation mechanisms deduced from AMS data in the Jaca-Pamplona basin (southern Pyrenees). *Physics and Chemistry of the Earth, 22*(1–2), 147–152.

Martín-HernándezHirt, F. A. M. (2003). The anisotropy of magnetic susceptibility in biotite, muscovite and chlorite single crystals. *Tectonophysics, 367*(1–2), 13–28.

Menzer, R. L., Bonnel, C., Gracia-Puzo, F., & Aubourg, C. (2024). Matrix deformation of marls in a foreland fold-and-thrust belt: The example of the eastern Jaca basin, southern Pyrenees. *Journal of Structural Geology, 182*, 105114. https://doi.org/10.1016/j.jsg.2024.105114

Millán, H., Pocoví, A., & Casas, A. (1995). El frente de cabalgamiento surpirenaico en el extremo occidental de las Sierras Exteriores: Sistemas imbricados y pliegues de despegue. *Revista De La Sociedad Geológica De España, 8*(1–2), 73–90.

Millán, H., Pueyo, E. L., Aurell, M., Luzón, A., Oliva, B., Martínez-Peña, M. B., & Pocoví, A. (2000). Actividad tectónica registrada en los depósitos terciarios del frente meriodinal del Pirineo Central. *Revista De La Sociedad Geológica De España, 13*, 279–300.

Mochales, T., Pueyo, E. L., Casas, A. M., Barnolas, A., & Oliva-Urcia, B. (2010). Anisotropic magnetic susceptibility record of the kinematics of the Boltaña Anticline (Southern Pyrenees). *Geological Journal, 45*(5–6), 562–581. https://doi.org/10.1002/gj.1207

Montes, M. J. (2009). Estratigrafía del Eoceno-Oligoceno de la Cuenca de Jaca. Sinclinorio del Guarga. *Colección De Estudios Altoaragoneses, 59*, 1–355.

Muñoz, J. A. (1992). Evolution of a continental collision belt: ECORS-Pyrenees crustal balanced cross-section. In K. R. McClay (Ed.), *Thrust Tectonics* (pp. 235–246). Chapman & Hall.

Muñoz, J. A. (2002). The Pyrenees. In W. Gibbons & T. Moreno (Eds.), *The geology of Spain* (pp. 370–385). The Geological Society.

Muñoz, J. A., Beamud, E., Fernández, O., Arbués, P., Dinarès-Turell, J., & Poblet, J. (2013). The Ainsa Fold and thrust oblique zone of the central Pyrenees: Kinematics of a curved contractional system from paleomagnetic and structural data. *Tectonics, 32*(5), 1142–1175. https://doi.org/10.1002/tect.20070

Muñoz, J. A., Mencos, J., Roca, E., Carrera, N., Gratacós, Ò., Ferrer, O., & Fernández, Ò. (2018). The structure of the South-Central-Pyrenean fold and thrust belt as constrained by subsurface data. *Geologica Acta: An International Earth Science Journal, 16*(4), 439–460. https://doi.org/10.1344/GeologicaActa2018.16.4.7

Mutti, E. (1991). Distinctive thin-bedded turbidite facies and related depositional environments in the Eocene Hecho Group (South-central Pyrenees, Spain). In *Deep-water turbidite systems* (pp. 181–205).

Nye, J. F. (1957). *Physical properties of crystals*. Oxford University Press.

Oliva-Urcia, B., Casas, A. M., Pueyo, E. L., & Pocoví, A. (2012). Structural and paleomagnetic evidence for non-rotational kinematics in the western termination of the External Sierras (southwestern central Pyrenees). *Geologica Acta, 10*(2), 125–144.

Oliva-Urcia, B., Larrasoaña, J. C., Pueyo, E. L., Gil-Imaz, A., Mata, P., Parés, J. M., Schleicher, A. M., & Pueyo-Anchuela, O. (2009). Complex magnetic subfabrics in a well-developed cleavage domain, Internal Sierras (Pyrenees, Spain). *Journal of Structural Geology, 31*, 163–176.

Oms, O., Dinarès-Turell, J., & Remacha, E. (2003). Magnetic stratigraphy from deep clastic turbidites: An example from the Eocene Hecho group (southern Pyrenees). *Studia Geophysica Et Geodaetica, 47*, 275–288. https://doi.org/10.1023/A:1023719607521

Parés, J. M. (2004). How deformed are weakly deformed mudrocks? Insights from magnetic anisotropy. *Geological Society, London, Special Publication, 238*, 191–203.

Parés, J. M. (2015). Sixty years of anisotropy of magnetic susceptibility in deformed sedimentary rocks. *Frontiers in Earth Science, 3*, 4. https://doi.org/10.3389/feart.2015.00004

Parés, J. M., van der Pluijm, B., & Dinarès-Turell, J. (1999). Evolution of magnetic fabrics during incipient deformation of mudrocks (Pyrenees, northern Spain). *Tectonophysics, 307*, 1–14. https://doi.org/10.1016/S0040-1951(99)00115-8

Payros, A., Astibia, H., Cearreta, A., Pereda-Suberbiola, X., Murelaga, X., & Badiola, A. (2000). The Upper Eocene South Pyrenean coastal deposits (Liedena Sandstone, Navarre): Sedimentary facies, benthic foraminifera and avian ichnology. *Facies, 42*, 19–23.

Payros, A., Pujalte, V., & Orue-Etxebarria, X. (1999). The South Pyrenean Eocene carbonate megabreccias revisited: New interpretation based on evidence from the Pamplona Basin. *Sedimentary Geology, 125*(3–4), 165–194.

Pedrera, A., García-Senz, J., Pueyo, E. L., López-Mir, B., Silva-Casal, R., & Díaz-Alvarado, J. (2023). Inhomogeneous rift inversion and the evolution of the Pyrenees. *Earth-Science Reviews, 245*, 104555. https://doi.org/10.1016/j.earscirev.2023.104555

Pocovi, A., Pueyo Anchuela, Ó., Pueyo, E. L., Casas-Sainz, A. M., Román Berdiel, M. T., Gil Imaz, A., Ramajo Cordero, J., Mochales, T., García Lasanta, C., Izquierdo, E., Parés, J. M., Sánchez, E., Soto Marín, R., Oliván, C., Rodríguez Pintó, A., Oliva-Urcia, B., & B., Villalaín, J. J. (2014). Magnetic fabrics in the Central-Western Pyrenees: An overview. *Tectonophysics, 629*, 303–318. https://doi.org/10.1016/j.tecto.2014.03.027

Pueyo Anchuela, Ó., Gil Imaz, A., & Pocoví Juan, A. (2010). Significance of AMS in multilayer systems in fold-and-thrust belts. A case study from the Eocene turbidites in the Southern Pyrenees (Spain). *Geological Journal, 45*(5–6), 544–561. https://doi.org/10.1002/gj.1194

Pueyo-Anchuela, O., Casas, A. M., Pueyo, E. L., Pocoví, A., & Gil-Imaz, A. (2013). Analysis of the ferromagnetic contribution to the susceptibility by low field and high field methods in sedimentary rocks of the Southern Pyrenees and Northern Ebro foreland basin (Spain). *Terranova, 25*(4), 307–314. https://doi.org/10.1111/ter.12037

Pueyo-Anchuela, O., Casas-Sainz, A. M., Pocoví-Juan, A., & Gil-Imaz, A. (2011). Lithology-dependent reliability of AMS analysis: A case study of the Eocene turbidities in the southern Pyrenees (Aragón, Spain). *Comptes Rendus Geoscience, 343*(1), 11–19. https://doi.org/10.1016/j.crte.2010.11.003

Pueyo-Anchuela, O., Pocoví-Juan, A., & Gil-Imaz, A. (2012a). Factors affecting the record of strain fabrics at the anisotropy of magnetic susceptibility: West-Central South-Pyrenean cleavage domain (Southern Pyrenees; NE Spain). *Tectonophysics, 554*, 1–17. https://doi.org/10.1016/j.tecto.2012.05.028

Pueyo-Anchuela, O., Pueyo, E. L., Casas-Sainz, A. M., Pocoví-Juan, A., & Gil-Imaz, A. (2012b). Vertical axis rotations in fold and thrust belts: comparison of AMS and paleomagnetic data in the Western External Sierras (Southern Pyrenees). *Tectonophysics, 532*, 119–133. https://doi.org/10.1016/j.tecto.2012.01.023

Pueyo-Morer, E. L., Millán-Garrido, H., Pocoví-Juan, A., & Parés, J. M. (1997). Determination of the folding mechanism by AMS data. Study of the relation between shortening and magnetic anisotropy in the Pico del Aguila anticline (southern Pyrenees). *Physics and Chemistry of the Earth, 22*(1–2), 195–201.

Puigdefábregas, C. (1975). La sedimentación molásica en la cuenca de Jaca. *Pirineos*, 104, 188 pp.

Puigdefábregas, C., Rojas Tapia, B., Sánchez Carpintero, I., & del Valle, J. (1974). Mapa geológico de la Hoja nº 142 (Aoiz). Mapa Geológico de España E. 1:50.000. Segunda Serie (MAGNA), Primera edición. IGME. Depósito legal: M-5.099-1978.

Rahl, J. M., Haines, S. H., & Van der Pluijm, B. A. (2011). Links between orogenic wedge deformation and erosional exhumation: Evidence from illite age analysis of fault rock and detrital thermochronology of syn-tectonic conglomerates in the Spanish Pyrenees. *Earth and Planetary Science Letters, 307*(1–2), 180–190. https://doi.org/10.1016/j.epsl.2011.04.036

Robador Moreno, A., Samsó Escolá, J. M., Ramajo Cordero, J., Barnolas Cortinas, A., Clariana García P., Martín Alfageme, S., & Gil Peña, I. (2024). Mapa Geológico Digital continuo E. 1: 50.000, Zona Pirineos Vasco-Cantábrica (Zona-1600). In *GEODE. Mapa Geológico Digital continuo de España [en línea]*. Disponible en: http://info.igme.es/cartografiadigital/geologica/geodezona.aspx?Id=Z1600

Rochette, P. (1987). Magnetic susceptibility of the rock matrix related to magnetic fabric studies. *Journal of Structural Geology, 9*(8), 1015–1020.

Rodríguez-Pintó, A., Pueyo, E. L., Serra-Kiel, J., Samsó, J. M., Barnolas, A., & Pocoví, A. (2012). Lutetian magnetostratigraphic calibration of larger foraminifera zonation (SBZ) in the Southern Pyrenees: The Isuela section. *Palaeogeography, Palaeoclimatology, Palaeoecology, 333–334*, 107–120.

Saspiturry, N., Razin, P., Baudin, T., Serrano, O., Issautier, B., Lasseur, E., Allanic, C., Thinon, I., & Leleu, S. (2019). Symmetry vs. asymmetry of a hyper-thinned rift: Example of the Mauléon Basin (Western Pyrenees, France). *Marine and Petroleum Geology, 104*, 86–105. https://doi.org/10.1016/j.marpetgeo.2019.03.031

Saur, H., Sénéchal, P., Boiron, T., Aubourg, C., Derluyn, H., & Moonen, P. (2020). First investigation of quartz and calcite shape fabrics in strained shales by means of X-ray tomography. *Journal of Structural Geology, 130*, 103905. https://doi.org/10.1016/j.jsg.2019.103905

Séguret, M. (1972). Étude tectonique des nappes et séries décollées de la partie centrale du versant sud des Pyrénées. Caractère synsédimentaire, rôle de la compression et de la gravité. Montpellier, *Publications de l'Université des Sciences et Techniques du Languedoc, Série Géologie Structurale, 2nd edition*, 150pp

Soto, R., Larrasoaña, J. C., Arlegui, L. E., Beamud, E., Oliva-Urcia, B., & Simón, J. L. (2009). Reliability of magnetic fabric of weakly deformed mudrocks as a palaeostress indicator in compressive settings. *Journal of Structural Geology, 31*(5), 512–522. https://doi.org/10.1016/j.jsg.2009.03.006

Tarling, D. H., & Hrouda, F. (1993). *The magnetic anisotropy of rocks*. London: Chapman Hall.

Tavani, S., Storti, F., Fernández, O., Muñoz, J. A., & Salvini, F. (2006). 3-D deformation pattern analysis and evolution of the Añisclo anticline, southern Pyrenees. *Journal of Structural Geology, 28*, 695–712. https://doi.org/10.1016/j.jsg.2006.01.009

Teixell, A. (1992). *Estructura alpina en la transversal de la terminación occidental de la zona axial pirenaica*. (Tesis Doctoral) Universidad de Barcelona.

Teixell, A. (1996). The Ansó transect of the southern Pyrenees: Basement and cover thrust geometries. *Journal of the Geological Society, 153*(2), 301–310.

Teixell, A. (1998). Crustal structure and orogenic material budget in the west central Pyrenees. *Tectonics, 17*(3), 395–406. https://doi.org/10.1029/98TC00561

Teixell, A., Labaume, P., & Lagabrielle, Y. (2016). The crustal evolution of the west-central Pyrenees revisited: Inferences from a new kinematic scenario. *Comptes Rendus Géoscience, 348*(3–4), 257–267. https://doi.org/10.1016/j.crte.2015.10.010

Toro, R., Izquierdo-Llavall, E., Casas, A. M., Rubio, F. M., Ayala, C., Martín-León, J., Clariana, P., Soto, R., Santolaria, P., Navas, J., Rey-Moral, C., Pueyo, E.L., & the 3DGeoEU WP6 Team. (2021). Harmonization procedure of the western Pyrenees using geological, gravimetric, petrophysical, and seismic data (Deliverable 6.1). GEOERA 3DGEO-EU, 3D Geomodeling for Europe, project number GeoE.171.005. *Project Report*, 90 pp.

Toro, R., Casas, A. M., Izquierdo-Llavall, E., Pueyo, E. L., Navas, J., Peropadre, C., & Martín, J. (2020). Geometría del basamento Pirenaico Suroccidental a partir de la exploración sísmica. *Geo-Temas, 18*, 565.

Vinyoles, A., López-Blanco, M., Garcés, M., Arbués, P., Valero, L., Beamud, E., Oliva-Urcia, B., & Cabello, P. (2021). 10 Myr evolution of sedimentation rates in a deep marine to non-marine foreland basin system: Tectonic and sedimentary controls (Eocene, Tremp-Jaca Basin, Southern Pyrenees, NE Spain). *Basin Research, 33*(1), 447–477.